Frontiers in Environmental Engineering

TYPE Original Research
PUBLISHED 19 September 2025
DOI 10.3389/fenve.2025.1641277

OPEN ACCESS

EDITED BY
Michael Fong,
National Institute of Standards and Technology,
United States

REVIEWED BY
Stephen F. Gonski,
University of Delaware, United States
Hong-Tao Cong,
Xiamen University, China

*CORRESPONDENCE
Allison M. Savoie,
allison.savoie@pnnl.gov

RECEIVED 04 June 2025
ACCEPTED 29 July 2025
PUBLISHED 19 September 2025

CITATION
Savoie AM, Ringham M, Torres Sanchez C, Carter BR, Dougherty S, Feely RA, Hegeman D, Herndon J, Khangaonkar T, Loretz J, Minck T, Pelman T, Premathilake L, Subban C, Vance J and Ward ND (2025) Novel field trial for ocean alkalinity enhancement using electrochemically derived aqueous alkalinity.
Front. Environ. Eng. 4:1641277.
doi: 10.3389/fenve.2025.1641277

Novel field trial for ocean alkalinity enhancement using electrochemically derived aqueous alkalinity

Allison M. Savoie[1]*, Mallory Ringham[2], Carolina Torres Sanchez[1], Brendan R. Carter[3,4], Sean Dougherty[4], Richard A. Feely[4], Dave Hegeman[2], Julian Herndon[3,4], Tarang Khangaonkar[1,5], Jeremy Loretz[2], Tyson Minck[2], Todd Pelman[2], Lakshitha Premathilake[1,5], Chinmayee Subban[1,6], Jesse Vance[2] and Nicholas D. Ward[1]

[1]Coastal Sciences Division, Pacific Northwest National Laboratory, Sequim, WA, United States, [2]Ebb Carbon, Inc., South San Francisco, CA, United States, [3]Cooperative Institute for Climate, Ocean, and Ecosystem Studies, University of Washington, Seattle, WA, United States, [4]Pacific Marine Environmental Laboratory, National Oceanic and Atmospheric Administration, Seattle, WA, United States, [5]Salish Sea Modeling Center, University of Washington, Tacoma, WA, United States, [6]Department of Materials Science and Engineering, University of Washington, Seattle, WA, United States

Ocean alkalinity enhancement is a proposed method of marine carbon dioxide removal that enhances the ocean's uptake of atmospheric carbon dioxide (CO_2) and converts it to dissolved bicarbonate for long-term ocean storage. This method of marine carbon dioxide removal has been gaining attention for its potential to durably (10,000+ years) store large amounts of CO_2 (Gt + where 1 Gt = 1×10^9 tons), while potentially ameliorating acidification in the vicinity of the alkalinity release. This study focuses on a novel release of electrochemically derived aqueous alkalinity into Sequim Bay, WA, through a previously established wastewater treatment plant (WWTP). This research was made possible through the collaboration of industry, academic, and federal partners, which enabled the establishment of an Ebb Carbon electrochemical mCDR system at the Pacific Northwest National Laboratory in Sequim, WA, for ocean alkalinity enhancement field trials. During these field trials, pH was measured across the WWTP system from the initial alkalinity dosing, throughout the WWTP, and at the outfall. We use the NBS scale for pH throughout this study as it is the scale used in discharge permit limits specified for WWTP and NPDES regulation and compliance monitoring. The background pH_{NBS} of Sequim Bay seawater was between 7.5 and 7.7 for the November and February field tests. The mixing tank's pH_{NBS} was raised to the maximum value permitted for the WWTP (9.0) and maintained across the system (±0.2) during the outfall releases. At the outfall, the elevated pH and alkalinity was quickly diluted, such that the region with a measurable signal was limited to within ~2.5 m of the discharge pipe. We were able to successfully monitor an increase in pH_{NBS} across all four pulses of alkalinity-enhanced seawater discharge during the February 2025 field trial, with peak pH_{NBS} values of 8.3 or 8.1, as recorded by outfall-adjacent YSI Exo 2 sonde and SAMI-pH sensors, respectively. The alkalinity-enhanced seawater did not measurably alter the surrounding waters' temperature, salinity, turbidity, or oxygen. This study provides proof-of-concept for a conservative small-scale release of electrochemically generated alkalinity-enhanced seawater from a coastal outfall.

KEYWORDS

marine carbon dioxide removal (mCDR), ocean alkalinity enhancement (OAE), coastal outfall, wastewater treatment (WWT) technologies, field experiment, ocean acidification

1 Introduction

Drastic reduction in carbon dioxide (CO_2) emissions supplemented with active removal of 100–1,000 Gt CO_2 from the atmosphere over the 21st century is necessary to limit global warming to below 2°C (UN, 2015; IPCC, 2018; Rogelj et al., 2018; IPCC, 2023). Among potential carbon dioxide removal (CDR) methods, marine geochemical approaches to capturing and storing CO_2 in seawater are gaining attention for their potential durability and ability to scale (Rau, 2011; National Academies of Sciences and Medicine, 2022; Cross et al., 2023). One promising approach to mCDR is ocean alkalinity enhancement (OAE) (Renforth and Henderson, 2017; Cai and Jiao, 2022; Oschlies et al., 2023; Cong et al., 2024). OAE is considered a promising potential approach for mCDR given its relatively low potential cost per ton of CO_2 removed from the atmosphere and potential to reach Gt-scale removal compared to other more expensive technologies like direct air capture (Cross et al., 2023). By elevating the alkalinity of seawater, OAE alters the speciation of dissolved inorganic carbon, and encourages the net transfer of CO_2 into the ocean either through an increase in net ocean CO_2 uptake or a reduction in net outgassing (Renforth and Henderson, 2017; Cai and Jiao, 2022; Schulz et al., 2023; Cong et al., 2024). The shifts lead to a durable (i.e., long-term) enhanced storage of ocean carbon relative to expectations without the OAE intervention, predominantly as elevated dissolved bicarbonate concentrations (Renforth and Henderson, 2017; Cai and Jiao, 2022; Schulz et al., 2023; Cong et al., 2024; Khangaonkar et al., 2024).

Multiple approaches to elevating seawater alkalinity have been proposed, including the addition of alkaline materials to seawater and the electrochemical conversion of seawater or brine into alkaline solutions that are delivered to the surface ocean (Cai and Jiao, 2022; Eisaman et al., 2023; Oschlies et al., 2023; Cong et al., 2024). The type of alkalinity and method of delivery impact the resulting chemical changes in the receiving seawater, but, in general, we expect an increase in pH and a rapid shift of dissolved inorganic carbon (DIC) speciation toward carbonate (CO_3^{2-}). This increase in pH, in turn, will also reduce the concentration of dissolved CO_2 gas in seawater ($pCO_{2(sw)}$) (Montserrat et al., 2017; Cai and Jiao, 2022; Eisaman et al., 2023; Hartmann et al., 2023; Schulz et al., 2023; Cong et al., 2024; Suitner et al., 2024). These changes are greatest near the point of alkalinity-enhanced seawater discharge and are diluted until the signal is indistinguishable from baseline variations (Khangaonkar et al., 2024; Hashim et al., 2025). Over weeks to years, $pCO_{2(sw)}$ re-equilibrates—or at least returns to values observed prior to alkalinity enhancement in regions where natural processes result in persistent disequilibria—due to changes in the net exchange of CO_2 across the air-sea boundary. Under typical ocean conditions, OAE results in an increase of 0.7–0.9 mol of DIC per mole of alkalinity added to seawater, though this value depends on the efficiency of alkaline delivery and air-sea equilibration. That is, the increases may be less when alkaline feedstocks do not fully dissolve or are added in regions where, for example, density currents drive alkalinity-enhanced seawater out of contact with the atmosphere (Fennel et al., 2023; He and Tyka, 2023; Ho et al., 2023; Wang et al., 2023; Khangaonkar et al., 2024; Ringham et al., 2024; Yankovsky et al., 2024; Zhou et al., 2024; Anderson et al., 2025). However, even if the alkalinity-enhanced seawater is out of contact with the atmosphere, it may still be beneficial for ameliorating ocean acidification in subsurface waters where applicable (Renforth and Henderson, 2017; Cai and Jiao, 2022; Oschlies et al., 2023; Bednaršek et al., 2025).

OAE is promising due to its potential scalability, the high durability of OAE CO_2 storage, and potential co-benefits, including the potential for local mitigation of seawater acidification (Renforth and Henderson, 2017; Cai and Jiao, 2022; Oschlies et al., 2023; Bednaršek et al., 2025). For these reasons, and in response to the urgency of developing climate solutions, efforts are simultaneously underway to research, test, and commercialize OAE technologies (National Academies of Sciences and Medicine, 2022; Palter et al., 2023; Carbon to Sea Intiative, 2024; Cross et al., 2024; Carbon to Sea Intiative, 2025; ICES, 2025; Travis, 2025; Yao et al., 2025). This study describes the deployment of a demonstration electrochemical OAE system as part of a collaboration between private (Ebb Carbon, Inc.), academic (University of Washington), and federal (Pacific Northwest National Laboratory; NOAA Pacific Marine Environmental Laboratory) partners, resulting in the dispersal of electrochemically generated aqueous alkalinity through a wastewater treatment plant (WWTP) at the Pacific Northwest National Laboratory (PNNL) into Sequim Bay, Washington, United States. The research conducted in this study was part of the NOAA-funded project EASE-OA (Electrochemical Acid Sequestration to Ease Ocean Acidification), which has included multiple components to advance towards OAE field trials, including: 1) testing and development of Ebb Carbon's electrochemical system; 2) simulation of continuous aqueous alkalinity-enhanced seawater discharge into Sequim Bay (Khangaonkar et al., 2024); 3) evaluation of the impact of aqueous alkalinity on local ecologically important eelgrass epifauna (Jones et al., 2024); and 4) monitoring CO_2 uptake in mesocosm-scale ex-situ experiments of seawater treated with aqueous alkalinity.

Ebb Carbon's approach to OAE is to utilize bipolar membrane electrodialysis (BPMED) to generate aqueous alkalinity from seawater that then returns to the surface ocean, while simultaneously removing acid from seawater (Eisaman et al., 2012; Eisaman, 2024). The minimum potential for reaction of water dissociation through BPMED compared to electrolysis is lower, 0.83 V versus 2.06 V (Eisaman et al., 2012; Eisaman et al., 2023; Kulkarni et al., 2024). Therefore, BPMED is a lower energy method for alkalinity production and in turn less expensive, which makes it an economically appealing option for OAE based CO_2 removal (Eisaman et al., 2012; Eisaman et al., 2023; Cross et al., 2024). The Ebb Carbon BPMED system in this study, designed to remove 100 t of atmospheric CO_2 yr^{-1}, began operating at PNNL-Sequim in August 2023. This system processes seawater sourced from Sequim Bay through the PNNL-Sequim facility to generate hydrochloric acid (HCl), sodium hydroxide (NaOH), and brine streams (Eisaman et al., 2012; Eisaman et al., 2023; Eisaman, 2024). The HCl produced is 0.5–1.0 mol L^{-1} and is utilized for PNNL-Sequim research focused on developing novel uses for the acid byproduct. While research is an efficient use of acid byproduct for a pilot scale BPMED implementation, the use for the larger quantities of HCl byproduct generated by scaled electrochemical OAE deployments is an active area of research. Potential use cases include algal cultivation, mineral extraction, and industrial applications (Eisaman et al., 2023; Eisaman, 2024; Hibbeln et al., 2024). The NaOH is mixed with the brine stream and remaining seawater for release back to the surface ocean. The enhanced alkalinity stream resulting from the Ebb Carbon system at PNNL-Sequim can vary in concentration from 0.2–1.0 mol L^{-1} NaOH and a practical salinity between 20–70. NaOH-based OAE research has been conducted in multiple laboratories (e.g., Hartmann et al., 2023; Iglesias-Rodríguez et al., 2023; Bach et al., 2024; Ferderer et al., 2024; Ringham et al., 2024; Britton et al., 2025), and a limited number of completed or planned field studies (i.e., Albright et al., 2016; Subhas et al., 2024), typically using the addition of 0.5–1 mol L^{-1} NaOH to raise seawater alkalinity.

While there is attention on the release of NaOH from ships for OAE research [i.e., LOC-NESS (Permit #EPA-HQ-MPRSA-2024–002)], the primary delivery method for electrochemically generated aqueous alkalinity in commercial projects is point source dispersal through a coastal outfall (Cai and Jiao, 2022; Cong et al., 2024). Within the US, coastal outfalls are regulated under the Clean Water Act, which requires National Pollutant Discharge Elimination System (NPDES) permits. Permits are tailored to specific provisions to ensure that any given pollutant discharge does not harm water quality or human health. Coastal outfalls are typically designed such that a released effluent quickly mixes into the natural environment. The initial discharge may have requirements for specific conditions (such as a maximum pH or concentration limit) by the ‘end-of-pipe’ before discharge into the natural environment or may include a mixing zone. A mixing zone is a regulatory concept used to specify a volume of receiving water centered on an outfall in which water quality standards may be temporarily exceeded, but by the edge of which the diluted effluent is indistinguishable from natural ambient conditions (EPA 820-B-14–004). Release of aqueous alkalinity through existing NPDES-permitted coastal outfalls and within the specified permit limits may be sufficient for compliance with existing standards, allowing for some OAE research. PNNL-Sequim has an onsite WWTP that is permitted for the release of wastewater within pH_{NBS} 6.0–9.0 at ‘end-of-pipe’. The permit allows WWTP discharge of seawater that is either treated with only enough alkalinity to remain within this pH range or with additional alkalinity and then allowed to re-equilibrate with atmospheric CO_2 and return to this range. As of this study, only one NPDES permit has been granted for an mCDR-specific process, specifically that of Ebb Carbon’s nearby Project Macoma pilot in Port Angeles, WA, which allows for routine discharge of alkalinity-enhanced seawater below pH_{NBS} 9.8 into a defined mixing zone (Permit #WA0991051). There are advantages to constraining alkalinity additions below pH_{NBS} 9.0, namely, adaptation to existing coastal outfalls permitted under this condition and limitations of concerns over environmental impacts and secondary precipitation. However, a lower pH maximum creates challenges for the release of aqueous alkalinity at increased scales, such as additional energy required to pump the seawater needed for dilution of the pH perturbation to the lower value or increased equipment and complexity required to pre-equilibrate alkalinity-enhanced seawater before release.

We released electrochemically generated aqueous alkalinity through the onsite WWTP at PNNL-Sequim into Sequim Bay, WA, in two experiments conducted in November 2024 and February 2025. Our first objective was to determine our ability to maintain, monitor, and deliver alkalinity-enhanced seawater through the multiple steps of the facility out to the outfall, and this objective was achieved. The second objective was to test our ability to detect the increased alkalinity from the outfall above ambient conditions, despite the upper pH_{NBS} limit of 9.0 and the presence of high tidal currents in this study area. Monitoring OAE in tidally energetic regions can be difficult due to rapid mixing and dilution effects, as well as large natural variability in carbonate chemistry due to these tidal fluctuations (Khangaonkar et al., 2024). Herein, we describe: 1) experimental design and release of alkalinity through the WWTP; 2) monitoring capabilities throughout the facility and extending beyond the coastal outfall; 3) near-field modeling results to estimate the dilution of the pH signal from the outfall. This study represents the first proof-of-concept of using existing coastal outfalls for electrochemical OAE research.

2 Materials and methods

2.1 Experimental design

PNNL-Sequim is located near the mouth of Sequim Bay, a semi-enclosed protected bay in the Salish Sea (Figure 1). Sequim Bay is a small and relatively undisturbed watershed with depths ranging from 5–30 m. Travis spit runs across the front of the bay, which creates a shallow, high current environment (Figure 1) (Khangaonkar et al., 2024). Average flow speeds are around 0.34 m/s for the bay and are driven primarily by tidal exchange (Harding and Harker-Klimes, 2017; Jones et al., 2019). Average ranges for salinity and temperature of the bay are 30–33 and 7°C–12.5°C, respectively (Jones et al., 2019). Generally, Sequim Bay acts as a CO_2 sink in the summer and as a CO_2 source in the winter months (Khangaonkar et al., 2024). The reported range in pH_{NBS} of Sequim Bay from Clallam County Environmental Health is from 7.2 to 8.3, with generally lower pH_{NBS} values in late summer to winter and higher values in late winter to mid-summer, as recorded by sensor measurements outside of Sequim Bay State Park and Johnson Creek (https://www.clallamcountywa.gov/1413/Trends-Monitoring-Data).

PNNL-Sequim facilities pump raw and filtered (40 μm) seawater from Sequim Bay and provide a filtered seawater source for Ebb Carbon’s BPMED system installed on site to generate aqueous

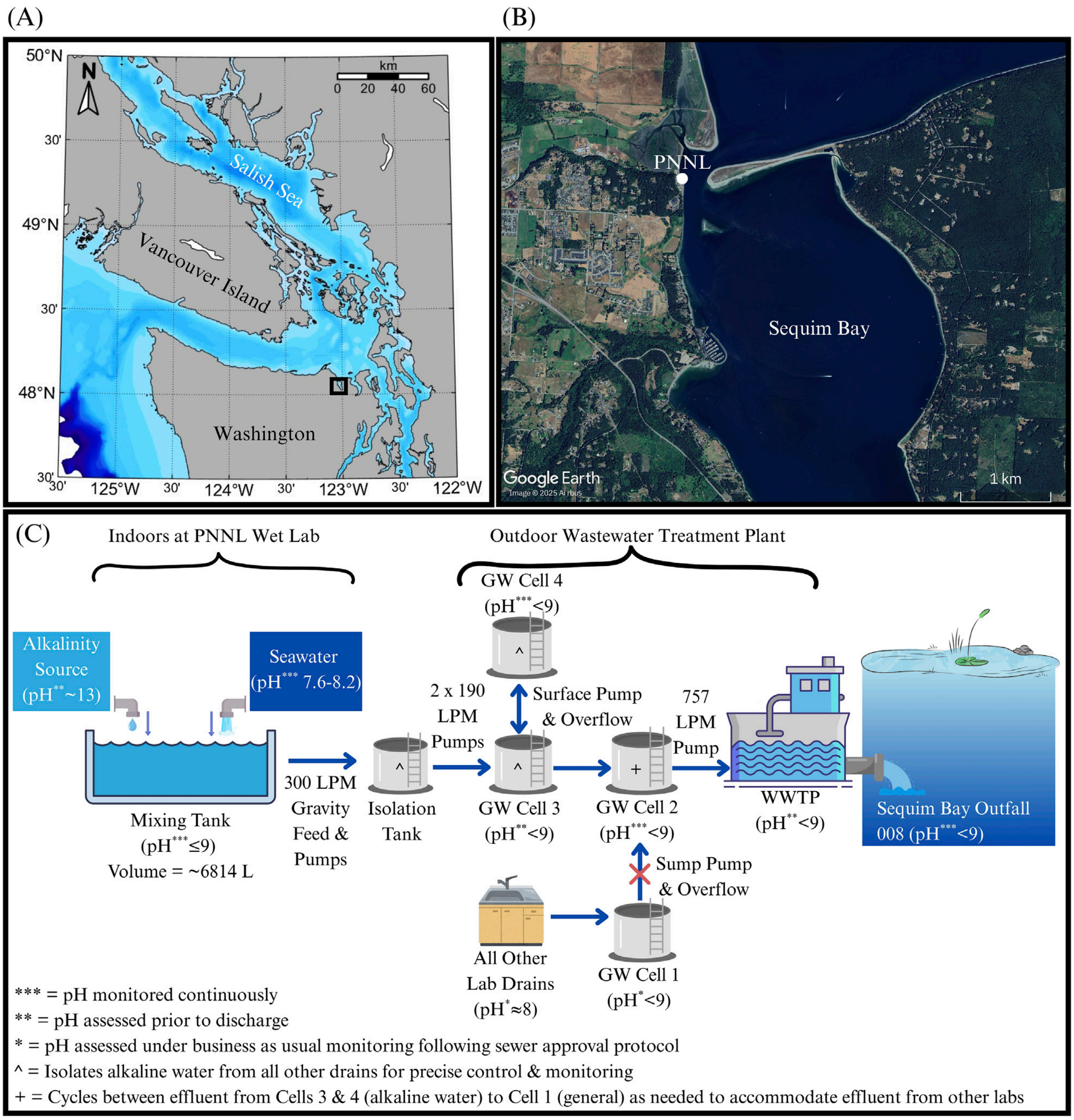

FIGURE 1
(A) Map of the greater Salish Sea region with a **(B)** focused view on our study region at PNNL at the mouth of Sequim Bay. The schematic in **(C)** details the steps of the alkaline feedstock dosing into seawater, followed by the flow through the facility, to the wastewater treatment plant at PNNL, and out the outfall into Sequim Bay. All pH values are indicated on the NBS scale.

alkalinity as described in Section 2.2. The facility uses four ~26,000 L groundwater holding cells (GW cells) to store and transfer wastewater from laboratories to the onsite wastewater treatment plant (WWTP). Wastewater from the WWTP is then pumped into Sequim Bay through a coastal outfall (Figure 1). GW Cells 1 and 2 receive wastewater from non-hazardous use of laboratory sink drains as well as specific drains in the facility's wet labs that use both fresh and seawater for a variety of experiments. GW Cell 2 is ultimately what gets pumped through the WWTP to Sequim Bay and can be either connected to or isolated from Cell 1. During the experiment pH was tightly controlled by isolating GW Cell 2, while the entire campus' wastewater generation that was unrelated to this test was directed to GW Cell 1. GW Cells 3 and 4 serve as additional isolation cells that can receive wastewater from specific wet lab drains in isolation from Cells 1 and 2 (as denoted by the red x in Figure 1). Water drained into Cells 3 and 4 is not automatically discharged to the bay until it is manually pumped into Cell 2. During the experiments, GW Cell 3 was continually filled with alkalized

TABLE 1 Water chemistry parameters during November field trial.

Location	Temp (°C)[a]	Salinity[a]	pH_{NBS}[a]	pCO_2 (µatm)[a]	TA (µmol/kg)[b]	DIC (µmol/kg)[b]	pH_T[c]
Baseline seawater	9.8–9.9	31.9–32.0	7.5–7.6	772–796	2,169–2,185 (n = 8)	2,103–2,130 (n = 8)	7.7–7.8 (n = 8)
Mixing Tank	9.9–10.2	30.1–30.3	8.9	70–110	2,983–3,099 (n = 6)	2,133–2,149 (n = 6)	8.8–8.9 (n = 6)
GW Cell 3	10.2–10.5	29.1–30.0	8.9	ND	2,868 (n = 1)	2,170 (n = 1)	8.8 (n = 1)
GW Cell 2	10.3–10.7	29.0–29.1	8.5	ND	2,750 (n = 1)	2,190 (n = 1)	8.6 (n = 1)
Outfall	9.3–9.7	28.9–29.2	7.8	600–1,150	ND	ND	ND
Pier	9.3–9.6	28.9–29.2	7.8–7.9	ND	ND	ND	ND

[a] Measured via sensors.

[b] Discretely analyzed from bottle samples.

[c] Calculated in CO2SYS, from bottle sample data.

ND = no data; n = number of samples collected; baseline seawater measured from raw seawater intake at PNNL using a Burke-O-Lator and bottle samples.

seawater and then transferred to GW Cell 2 after confirming permit compliance. Cell 4 remained empty, serving as a fail-safe should any abnormalities occur. This design facilitated the monitoring of pH throughout the facility to ensure pH levels were in compliance prior to discharge.

Downstream of GW Cell 2, the WWTP effluent is processed with various filters and treatments before discharge. In order, these include: a bag filter, UV treatment, a granulated activated carbon (GAC) filter, a second bag filter, and finally a second-stage UV treatment. The design of this WWTP is not intended to treat water for pH adjustment in these final filtration steps. However, it is possible that pH will decrease slightly as it travels through the final components of the system due to continued equilibration with air. However, this decrease is likely minimal compared to equilibration that occurs when moving water between the groundwater cells. The GW cells are open to the atmosphere and the water is substantially bubbled when pumped between each cell like a waterfall, which is why they are continuously monitored throughout the experiment. The filter system is not open to the atmosphere like the GW cells. This system, which typically discharges ~40,000 L d^{-1} to Sequim Bay depending on lab use, was leveraged for the ability to precisely monitor water quality, particularly pH, between groundwater holding cells. This allows for the release of alkalinity-enhanced seawater with minimal risk of approaching regulatory water quality limits for this site. The outfall (Sequim Bay Outfall 008) is a 20 cm flanged pinch valve located ~5–8 m below the water's surface within ~40 m of the seawall near the laboratory (48° 4′43.00″N, 123° 2′42.00″W) (Figure 1). However, the depth and distance from shore can vary based on high or low tide conditions, as this site has a ~3 m tidal range.

November and February were chosen for these initial trials for two reasons. First, natural variability of pCO_2 and pH in Sequim Bay is substantially lower in winter months compared to summer, making our odds of detecting the alkaline discharge higher in the winter (Evans et al., 2019). Second, the presence of juvenile salmon in nearshore areas peaks in the summer (US EPA, 2021). As we were initially uncertain how far the plume would extend, we conducted our preliminary experiments during a time of year when this sensitive endangered species was unlikely to be present. Over the course of 1 day each during two discrete alkalinity enhancement experiments on 7 November 2024, and 7 February 2025, aqueous alkalinity was continually mixed into a ~6800 L flow-through seawater mixing tank, raising seawater pH_{NBS} from ambient conditions (7.5–7.7; Tables 1, 2) to <9.0. The alkalinity-enhanced seawater was then delivered to an intermediate isolation tank through a combination of gravity feeding and pumping. From this tank, it was actively pumped to GW Cells 3 and then 2 before reaching the WWTP to be discharged through Sequim Bay Outfall 008. Discharged effluent from this process was continuously monitored within the mixing tank, GW Cells 3 and 2, at the coastal outfall, and from a nearby pier, as described in Sections 2.2, 2.3.

2.2 Alkalinity generation

Alkalinity was generated using filtered Sequim Bay seawater processed through an Ebb Carbon BPMED system (Figure 2) (Eisaman et al., 2023; Eisaman, 2024; Khangaonkar et al., 2024). The process consists of seawater treatment with operations representative of a commercial desalination plant. The seawater passes through mixed media filters, including granulated activated carbon (GAC) and sand filters. The water is then treated with nanofiltration (NF) to separate divalent ions (magnesium (Mg^{2+}), calcium (Ca^{2+})), creating a permeate and concentrate stream. The NF concentrate goes to the lab drain, and the NF permeate continues in the process. This water then undergoes reverse osmosis (RO), which creates a brine concentrate and RO permeate feed. Both of these streams feed the BPMED process and while pH can vary during this process, it generally remains near ambient seawater conditions (~7–8). Within the BPMED process, sodium chloride (NaCl) and water (H_2O) are dissociated to form HCl (0.5–1.0 mol L^{-1}) and NaOH (0.5–0.75 mol L^{-1}). The product streams are stored for use in mesocosm experiments, for neutralization discharged through the PNNL-Sequim WWTP, or further research on productive uses for low-carbon acid. For the alkalinity-enhanced seawater discharges in November 2024 and February 2025, the BPMED system generated approximately 1,000 L of acid and 1,000 L of base during the month leading up to each experiment. The acid and base were stored in closed 1,000 L intermediate bulk containers (IBC) until the beginning of each alkalinity-enhanced seawater discharge.

During the November 2024 discharge, base product was dispersed evenly over time to the mixing tank and mixed with seawater (Figure 3). A total of 50 L of base product (0.8 mol L^{-1}) was

TABLE 2 Water chemistry parameters during February field trial.

Location	Temp (°C)^a	Salinity^a	pH_{NBS}^{a}	pCO_2 (μatm)^a	TA (μmol/kg)^b	DIC (μmol/kg)^b	pH_T^{c}
Baseline seawater	7.3–7.9	31.3–31.5	7.6–7.7	ND	2,150–2,156 (n = 6)	2089–2098 (n = 6)	7.8 (n = 6)
Mixing Tank	6.9–7.2	30.9–31.0	8.9–9.1	35–52	3,212–3,314 (n = 6)	2095–2,135 (n = 6)	9.1–9.2 (n = 6)
GW Cell 3	6.5–7.2	30.1–31.1	9.0	ND	3,191–3,279 (n = 3)	2,126–2,155 (n = 3)	9.1–9.2 (n = 3)
GW Cell 2	6.9–7.8	31.8–32.0	8.6–8.9	ND	2,899–3,194 (n = 4)	2,127–2,145 (n = 4)	8.8–9.0 (n = 4)
Outfall	6.7–8.1	31.0–31.5	7.5–8.3	464–875	ND	ND	ND
Pier	6.7–7.6	31.3–31.8	7.9–8.0	ND	2,154–2,155 (n = 3)	2089–2095 (n = 3)	7.8 (n = 3)

[a] Measured via sensors.

[b] Discretely analyzed from bottle samples.

[c] Calculated in CO2SYS, from bottle sample data.

ND = no data; n = number of samples collected; baseline seawater measured from raw seawater intake at PNNL using a Burke-O-Lator and bottle samples.

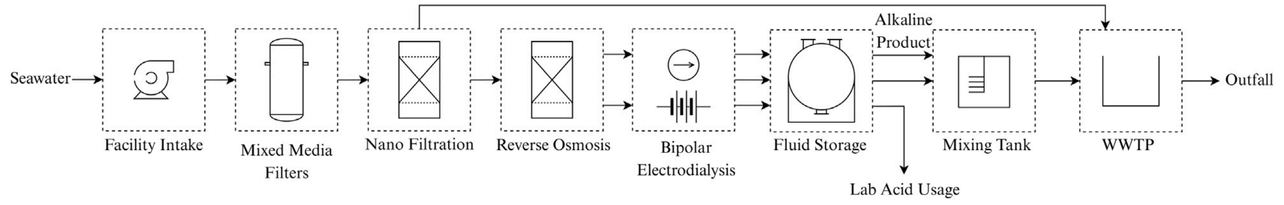

FIGURE 2
Schematic of Ebb Carbon processing steps for producing the aqueous alkaline feedstock, including pretreatment operations representative of those used in commercial desalination.

mixed into seawater in the mixing tank and subsequently released through the WWTP and outfall over 40 min (15:53–16:33) at a rate of ~655 L min^{-1}, resulting in a total release of ~26,200 L of alkalinity-enhanced seawater (Figure 3; Supplementary Table S1). During the February 2025 discharge, the base was introduced to the mixing tank with seawater prior to the discharge and then continuously through the experiment to maintain a 9.0 pH in the mixing tank. A total of 381 L of base product (0.66 mol L^{-1} NaOH) was mixed into seawater in the mixing tank and subsequently released through the WWTP and outfall over four separate pulses that all occurred on February 7 between 9:20 to 17:06 (Figure 3; Supplementary Table S1). All pulses discharged at a rate of around 656 L min^{-1}. Total volume of seawater discharged and time for each pulse were: 59,000 L from 9:20–10:50 (90 min), 52,200 L from 11:50–13:10 (80 min), 43,200 L from 14:09–15:15 (66 min), and 26,000 L from 16:26–17:06 (40 min) (Figure 3; Supplementary Table S1). The total volume for the release in February was ~180,300 L over 276 min of total release time (Supplementary Table S1).

The variable length in pulses between November and February were due to a couple different variables. The 40-min pulse in November is the length of time it takes to pump out GW Cell 2 when we're not constantly filling it (i.e., in November we just filled it up once and turned off our mixing tank). November was limited to one pulse as this was a targeted pilot experiment to assess operational control and detectability at the outfall. This trial indicated the output of alkalinity-enhanced seawater was constrained by rates of draining the mixing tank (gravity fed) and filling the tank with raw seawater to mix with base product. To increase these rates for the February trial, pumps were added to drain the mixing tank (no longer gravity fed, see Figure 1) and we modified the wet lab plumbing to increase the rate of raw seawater input. These modifications enabled the larger scale release in February. Additionally, the successful demonstration of permit compliance in November and the limited environmental detectability of the signal provided further assurance that a larger scale release was merited. The variable pulse lengths in February are from constantly refilling GW Cell 2, while still discharging from it. The first pulse was the longest because we had the highest water pressure for the seawater intake earliest in the day. Throughout the day, our water pressure for the seawater intake decreased so we could not fill GW Cell 2 as quickly later in the day. For the final pulse, we turned off the water completely so it was more or less identical to November's pulse length.

2.3 Monitoring and data processing

Throughout the system, physical and chemical parameters were measured to 1) assess pH of the alkaline seawater solution while moving through the wastewater treatment system, ensuring compliance with permitted WWTP discharge; and 2) evaluate the ability to identify and monitor the alkaline release in the natural environment at the outfall and nearby pier.

Continuous measurements of salinity and temperature of the baseline seawater conditions were made using a MultiLab IDS 4310 YSI probe on a Burke-O-Lator system that analyzes seawater from the raw intake line (Campbell et al., 2023). The addition of aqueous alkalinity to flow-through seawater in the

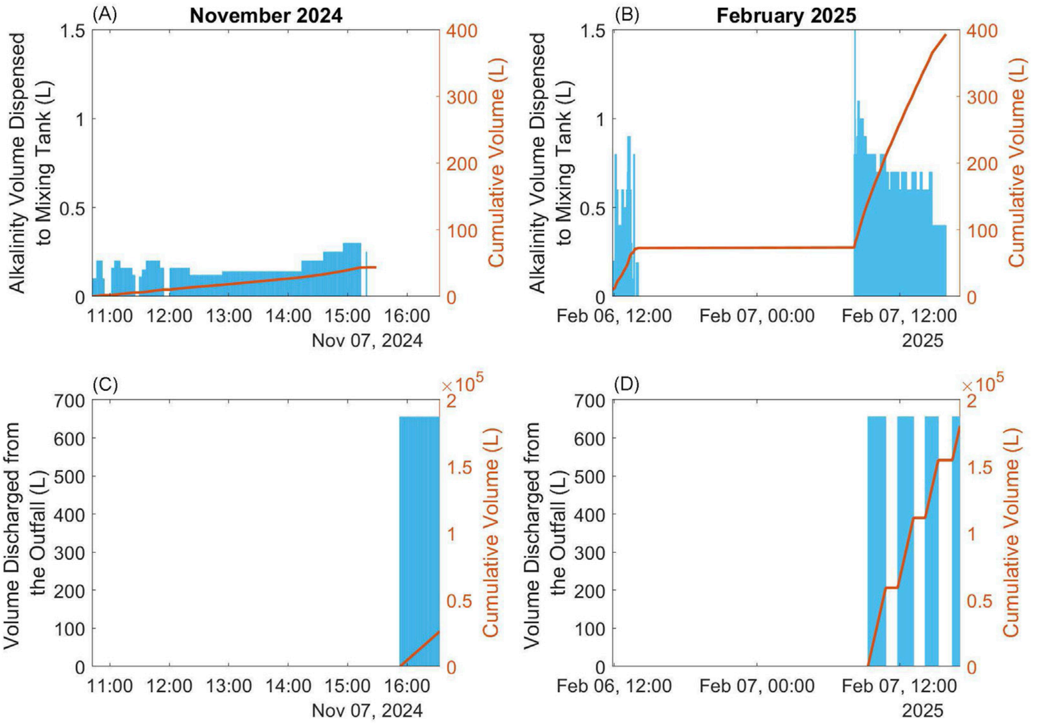

FIGURE 3
Volume (L) of alkalinity feedstock used for **(A)** November and **(B)** February trials. Volume (L) of alkalinity-enhanced seawater discharged into the Bay in **(C)** November and **(D)** February trials.

mixing tank was monitored during both the November 2024 and February 2025 experiments by measuring the time and rate of flow as base was pumped from the storage IBC into the mixing tank. The mixing tank was equipped with an ASVCO$_2$ system to record the mole fraction of CO$_2$ every 30 min, which is the minimum processing time between samples (Sutton et al., 2014). The mole fraction of CO$_2$ was then used to calculate pCO$_2$ for the mixing tank during the experiment (Sutton et al., 2014). YSI Pro DSS sondes were deployed to monitor seawater temperature, salinity, turbidity, dissolved oxygen (DO), and pH$_{NBS}$ every minute within- 1) the flow-through mixing tank; 2) GW Cell 3; and 3) GW Cell 2. YSI Exo 2 sondes were deployed to monitor seawater temperature, salinity, turbidity, dissolved oxygen (DO), and pH$_{NBS}$ every minute at two locations- 1) on a cage deployed by divers immediately in front of the WWTP outfall and 2) hanging at 2 m depth from the pier, ~70 m away from the outfall (November only) (Figures 1, 3). A Seabird Hydrocat EP-V2 was deployed from the pier in February instead of a YSI Exo2 sonde and collected measurements every 3 min on the first day and then every 10 min on the following days to ensure battery life for the experiment. We acquired and utilized the Seabird Hydrocat EP-V2 in February because it has higher accuracy than that of the YSI Exo2. A Sunburst SAMI-CO$_2$ sensor was deployed at the outfall during both the November and February experiments, which collected data every hour in November and every 30 min in February for higher resolution (DeGrandpre et al., 1995; Lai et al., 2018). A SAMI-pH sensor was added to the outfall cage and the pier station for the February 2025 experiment and collected data every 15 min (Seidel et al., 2008; Lai et al., 2018). The SAMI-pHs were added for February in part to get high accuracy pH readings that the YSI Exo2 sondes are not capable of. Secondly, we adjusted our experimental design to add SAMI pHs since we had difficulty detecting a signal in November's field trial. The SAMI CO$_2$ and SAMI pH have a minimum sample collection period of 15 min due to sample processing and response times, which is why they collected samples less frequently than the sondes. The range in salinity, temperature, pH$_{NBS}$, pCO$_2$, as recorded by the sensors is included in Tables 1, 2. The range in pH$_{NBS}$ data reported at the outfall includes data from both the YSI Exo2 and SAMI pH. The details for the instuments utilized, their deployment locations, and sampling intervals for the November and February field trials are reiterated in Supplementary Tables S2, S3.

The YSI sondes were calibrated using Orion pH$_{NBS}$ 4.01, 7, and 10.01 buffers. The YSI Exo2 sondes deployed at the outfall were calibrated 6 days in advance of the November alkaline release and within 24 h of deployment before the February release, while the Pro DSS sondes were calibrated the day of the alkalinity release. The YSI Exo2 sonde was calibrated in further advance in November's field trial due to diver availability for deployment of the sensors near the outfall. It remained off underwater until it was programmed to collect data, similar to the SAMIs. All YSI sondes measured pH at ± 0.1 accuracy and ±0.01 resolution. The Seabird Hydrocat EP-V2 was calibrated for pH immediately before deployment at the pier using 3 colorless NBS buffers (4.01, 7.0, 10.01). This sensor had an estimated accuracy of ±0.1 and a resolution of 0.01 units. The SAMI-CO$_2$ and SAMI-pH sensors were calibrated annually following manufacturer recommendations by Sunburst Sensors. The SAMI-CO$_2$ collected measurements at an estimated accuracy of ±3 µatm and precision of 1 µatm. The SAMI-pH sensors collected measurements at an accuracy of ±0.003 units and precision of 0.001 (in total scale). SAMI-pH data was processed using salinity data from the sondes deployed alongside them using the QC_pH program from Sunburst Sensors. YSI sondes and Seabird Hydrocat EP-V2 sensors output pH on the NBS scale by default. SAMI-pH data is on the total scale, therefore these values were input to CO2SYS to convert them to the NBS scale for comparison with the other sensors (Sharp et al., 2020). On average, the pH was 0.10 (±<0.001) higher on the NBS scale than on the total scale for our seawater conditions based on the calculations from CO2SYS of the sensor measurements. We used individually calculated CO2SYS values for every measurement instead of an average offset as this value can vary slightly based on a number of factors.

Along with these sensors, discrete water samples for dissolved inorganic carbon (DIC) and total alkalinity (TA) analysis were periodically collected from the raw seawater line and mixing tank from beginning to end of the experiment following standard methods outlined in Dickson et al. (2007). There were also discrete samples occasionally collected from GW Cell 2, GW Cell 3, and the pier following the same methods during the discharge periods only. No samples were collected at the outfall since it was not accessible for grab samples using the same methods. We did not expect or observe any secondary precipitation of carbonate minerals during this study, either in the mixing tank where the base product is first mixed with seawater or at the outfall, due to the low pH limits and rapid dilution of the alkaline product by seawater (Ringham et al., 2024; Suitner et al., 2024). While it is common for brucite to form under initial addition of base product, it often redissolves quickly with mixing as long as thresholds for "runaway precipitation" are not exceeded (Moras et al., 2022; Ringham et al., 2024; Suitner et al., 2024; Suitner et al., 2025). We ensured the solution was well mixed in the mixing tank before passing to any of the GW Cells. DIC was analyzed on an Apollo SciTech Dissolved Inorganic Carbon Analyzer (Model: AS-C6L), and TA was analyzed on an Apollo SciTech Total Alkalinity Titrator (AS-ALK3), referenced against certified reference materials (CRMs) supplied by the Dickson laboratory at Scripps Institution of Oceanography. The precision based on the repeated measurement of CRMs during sample analysis for TA and DIC was determined to be ±1 μmol kg^{-1} for both parameters.

Carbonate chemistry, including pH, was calculated from these DIC and TA samples using the MATLAB version of CO2SYS (Sharp et al., 2020). The pH was calculated from DIC and TA sample data in both NBS and total scale, as total scale is the standard for oceanographic research and sample data reporting, using K_1 and K_2 dissociation constants from Lueker et al. (2000), which is more optimal for pH_T, and Cai et al. (1998), which is more optimal for pH_{NBS}. The average offset from discrete samples analyzed using CO2SYS was also 0.10 (±0.003) when using either the set of K_1 and K_2 dissociation constants at the range of temperatures and salinities in this study. Since pH_T is standard for oceanographic samples, it is reported in Table 1 with values calculated from the Lueker et al. (2000) constants. Other constants remained the same for both calculations which include the KSO_4 dissociation constant from Dickson (1990), KF dissociation constant from Perez and Fraga (1987), and borate-to-salinity ratio from Lee et al. (2010). Organic alkalinity was estimated using the DIC values from the pier discrete samples in February (n = 3) and pH sensor data from the SAMI pH using methods from Fassbender et al. (2017). We note that for the ocean acidification community, this is referred to as excess alkalinity as opposed to organic alkalinity when the functional groups are uncharacterized (Sharp and Byrne, 2021). However, in the OAE community, excess alkalinity can refer to alkalinity delivered above biogeochemical thresholds for secondary, abiotic precipitation and thus, we will use "organic alkalinity" to avoid confusion. Based on this very limited sample set, organic alkalinity seems to have a very small impact (2.7 μmol kg^{-1} ± 1.7 μmol kg^{-1}) on the total alkalinity for this study. All figures (except Figure 8 which is detailed in the next section) were generated using Google Earth (Figure 1), Canva (Figures 1, 2, 4), and MATLAB (Figures 3, 5–7, Supplementary Figures S1-S11), utilizing the CO2SYS (Sharp et al., 2020), M_Map (Pawlowicz, 2020), QC_pH (Sunburst Sensors), and cmocean (Thyng et al., 2016) packages in MATLAB. Outlier filtering was done using the "isoutlier" function in MATLAB for the sonde seawater salinity and temperature data. Additional parameters that may be of interest are included in the supplementary figures, which include temperature, salinity, pH_{NBS}, turbidity, dissolved oxygen, and pCO_2 (when measured) for each step along the WWTP (Supplementary Figures S2-S11).

2.4 Near-field modeling

In the immediate vicinity of the outfall, the plume dynamics of the discharged water are primarily governed by the flow momentum and buoyancy. The plume undergoes intense turbulent mixing while interacting with the surrounding ambient currents during this initial phase, which is called the near-field or zone of initial dilution (Roberts, 1990; Baumgartner et al., 1994). It is challenging to capture/characterize the near-field of a plume using grid-based hydrodynamic circulation models due to limitations in operational spatial scales. To address this limitation, we used grid-less near-field plume dilution models based on (1) the length-scale approach and (2) the integral modeling approach. The near-field modeling for this study was conducted using PLUMES2.0, which is a three-dimensional Lagrangian integral plume model (Khangaonkar et al., 2024). PLUMES2.0 is a re-development of its predecessor UM3, which has been widely used for dilution modeling needs of the NPDES permitting process. The CO2SYS module was integrated into PLUMES2.0 to simulate the alkalinity release and the associated changes to the carbonate chemistry of the plume. This allowed the computation of the spatial distribution of pH_T, DIC, and TA along the near-field plume trajectory for monitoring, reporting, and verification (MRV) and other OAE-based mCDR system design purposes. The pH_{NBS} was then calculated by applying the offset of 0.10 calculated previously (Section 2.3).

PLUMES2.0 is a quasi-steady state model that operates under the assumption of steady state ambient conditions during the dynamic plume evolution phase. The diffuser/outfall characteristics (port diameter, port depths, orientation, etc.) need to be provided as user inputs, together with ambient conditions such as currents and stratification (salinity and temperature profiles). PLUMES2.0 was applied to simulate two model scenarios corresponding to the first two pulses of alkalinity release conducted at Sequim Bay outfall in February. Release 1 simulated

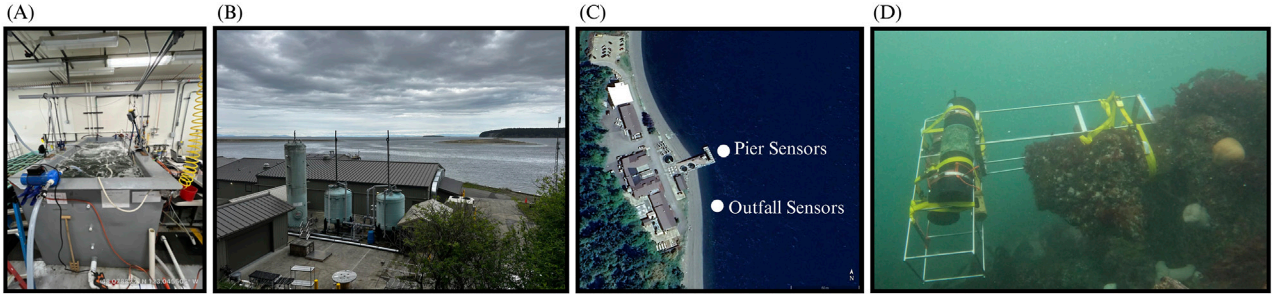

FIGURE 4
(A) Mixing tank equipped with sensors for continuous monitoring. **(B)** Outdoor wastewater treatment plant tanks. **(C)** Location of sensors for continuous measurement of water at the outfall and the nearby pier. **(D)** *In situ* photos of the sensors deployed on the outfall during the February 2025 alkalinity release.

the first pulse from 9:20–10:50 at a flow rate of 656 L m^{-1}, and release 2 simulated the second pulse from 11:50–13:10 at 653 L m^{-1}. The ambient currents for each release scenario were obtained from the Salish Sea and Columbia River operational forecast system (SSCOFS) model (Supplementary Figure S12), and the ambient pH, DIC, and TA were acquired from the measurements at the Marine and Coastal Research Laboratory (MCRL) Data monitoring station in Sequim Bay maintained by PNNL. The initial pH and TA values for the alkalinity releases were obtained from the measurements conducted at GW Cell 2 prior to release (Table 2). The PLUMES2.0 model results are detailed in Figure 8; Supplementary Figure S13.

3 Results

As a first trial, the November 2024 alkalinity-enhanced seawater release was used to test our ability to monitor and maintain an elevated $pH_{NBS} \leq 9.0$ while remaining within compliance of water quality standards at the outfall. The initial temperature, salinity, and pH_{NBS} of seawater at the beginning of the alkaline release ranged from 9.8°C–9.9°C, 31.9–32.0, and 7.5–7.6, respectively (Table 1). pH_{NBS} was increased to 9.0 from ambient conditions of 7.5–7.6 within the mixing tank (Supplementary Figures S2, S5). The pCO_2 in the mixing tank decreased from ambient conditions of 772–796 µatm to 70–110 µatm in November, as measured by the $ASVCO_2$ system (Table 1). The alkalinity enhanced seawater was pumped into GW Cell 3, where pH_{NBS} was observed at 8.9, with the slight reduction likely due to mixing with residual water remaining within the cell (Supplementary Figures S3, S5). pH_{NBS} again decreased within GW Cell 2 to 8.7, which was released from the WWTP outfall (Supplementary Figures S4, S5). The pH_{NBS} at the outfall during and after the alkaline release did not deviate from ambient conditions (Supplementary Figures S5, S5), indicating that sensors deployed on the outfall pipe were either not located in line with the alkalinity-enhanced seawater discharged or the pH_{NBS} signal was diluted too rapidly to be captured at this point. No alkaline signal was determined at the pier, however there was a flood tide during this time that could have diverted water into the Bay away from the pier rather than toward the inlet (Supplementary Figures S6, S5). A comparison of results from the YSI sondes and pH calculated from DIC/TA samples (on total and NBS scale) within the mixing tank and GW cells indicated that the sondes slightly underestimated pH (Table 1). However, the final release of alkaline seawater at the outfall remained at $pH_{NBS} < 9.0$ and within regulatory monitoring requirements, even if we adjust for the apparent measurement bias. While pH calculated from DIC and TA is potentially more accurate than measuring with a sonde, this is not practical from a compliance monitoring standpoint, given that the analysis of samples is often delayed resulting in limited usefulness in real-time decision making.

The second alkalinity-enhanced seawater release in February 2025 (~180,300 L) was ~6.9x larger than the volume released in November 2024 (~26,200 L) and was discharged into Sequim Bay during four separate pulses through the WWTP (Figure 3). The initial temperature, salinity, and pH of seawater at the beginning of the alkaline release ranged from 7.3°C–7.9°C, 31.3–31.5, and 7.6–7.7, respectively (Table 2). pH_{NBS} was increased to 8.9–9.1 from ambient conditions of 7.6–7.7 within the mixing tank (Supplementary Figures S7, S6). For the February trial, seawater pCO_2 data was not recorded by the $ASVCO_2$ system in the mixing tank prior to base addition. Therefore, the ambient conditions were estimated using the range in pCO_2 from the SAMI-CO_2 at the outfall within 12 h prior to the start of the experiment. Based on the SAMI-CO_2 and $ASVCO_2$ data, the baseline pCO_2 was between ~812 and 846 µatm, which decreased to 35–52 µatm (Table 2; Supplementary Figure S10). The pH_{NBS} was maintained through GW Cells 3 and 2 at 9.0 and 8.5–9.0, respectively, across all four pulses of alkalinity-enhanced seawater discharge (Supplementary Figures S6, S8, S9). The decrease at the end of the final pulse is likely due to GW Cell 2 no longer receiving alkalinity-enhanced water from GW Cell 3. Again, pH measured via YSI sondes was lower than that calculated via CO2SYS from DIC/TA samples in the mixing tank and GW cells (Table 2). However, the final release of alkaline seawater at the outfall remained <9.0, within regulatory monitoring requirements (Supplementary Figures S10, S6). In contrast to the November trial, there was a detectable increase in pH_{NBS} at the outfall over the four pulses during the February trial. During all four pulses, the Bay was in high tide conditions with a slight increase in water surface elevation over the day (Supplementary Figure S1).

Temperature, salinity, and pH_{NBS} were measured continuously for a week at the outfall and pier, beginning 3 days before the

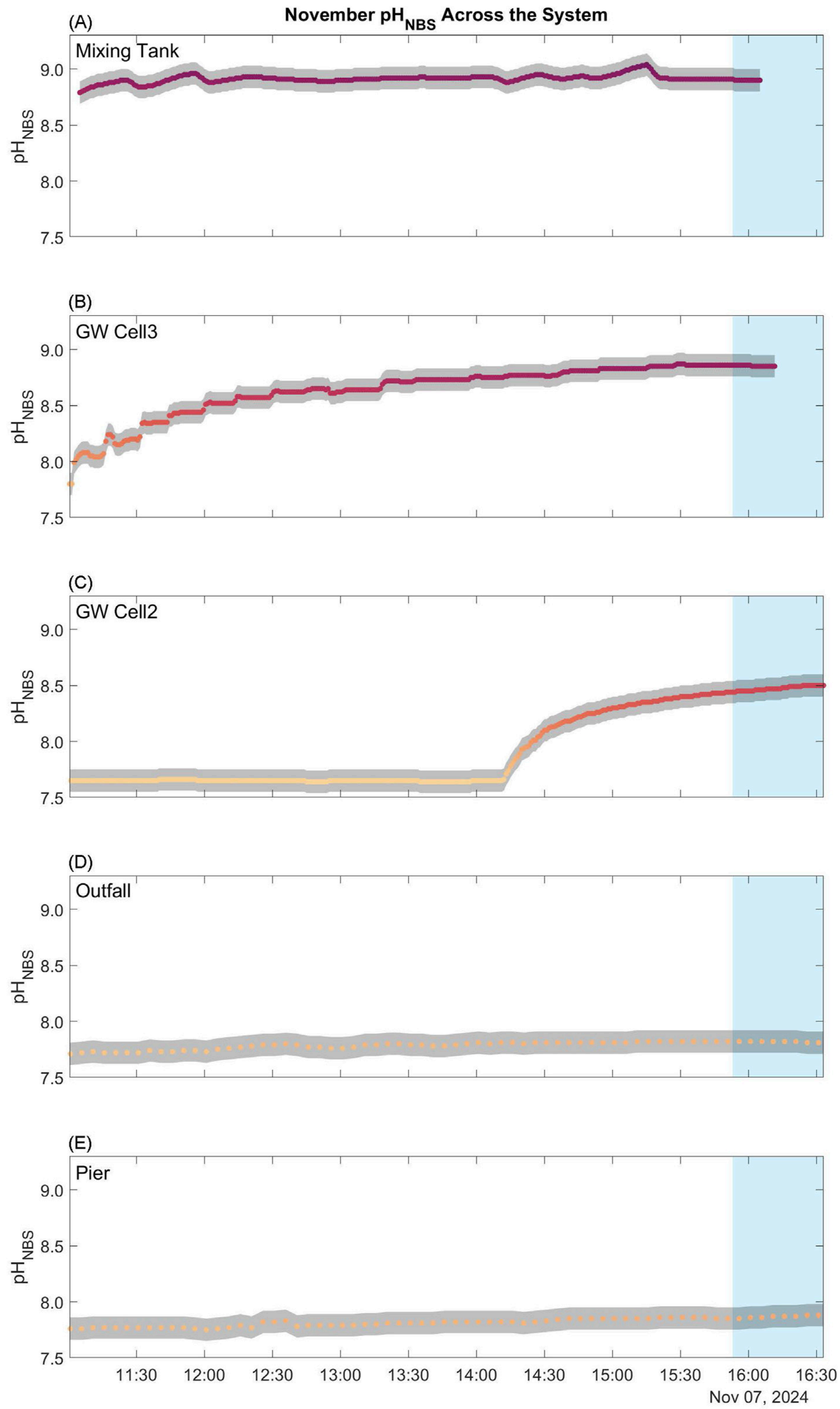

FIGURE 5
pH$_{NBS}$ data collected on the day of the November field trial across the **(A)** mixing tank, **(B)** GW Cell 3, **(C)** GW Cell 2, **(D)** Outfall, and **(E)** Pier. Lighter color points are lower pH, while darker colors indicate higher pH. Gray shading indicates the measurement uncertainty associated with each parameter. Blue boxes indicate the periods where alkalinity was discharged into Sequim Bay.

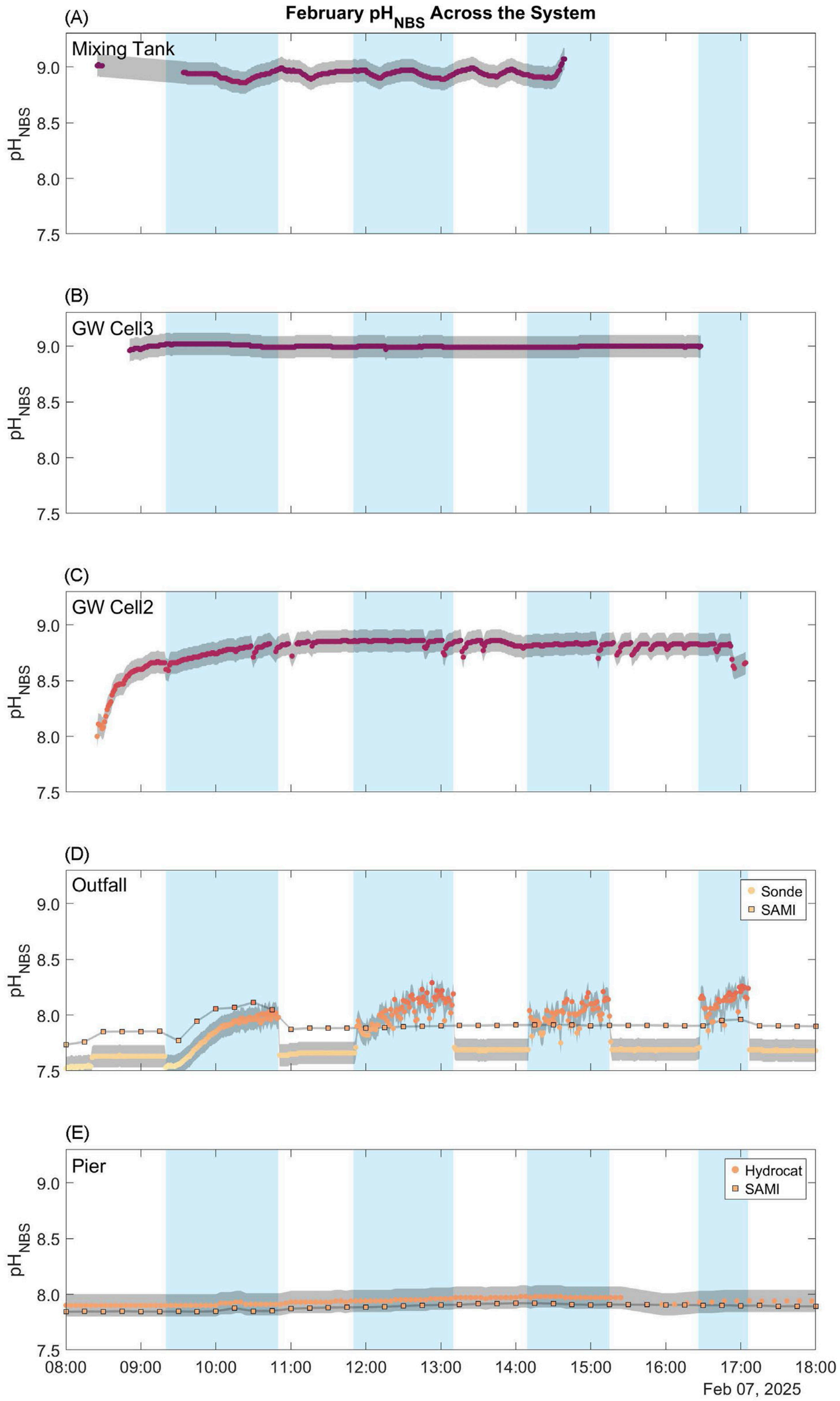

FIGURE 6
pH_{NBS} data collected on the day of the February field trial across the **(A)** mixing tank, **(B)** GW Cell 3, **(C)** GW Cell 2, **(D)** Outfall, and **(E)** Pier. Circles indicate data collected by the sondes or the Hydrocat at the pier. Squares are data collected from the SAMI pHs. Lighter color points are lower pH, while darker colors indicate higher pH. Gray shading indicates the error associated with each parameter. Blue boxes indicate the periods where alkalinity was discharged into the Bay.

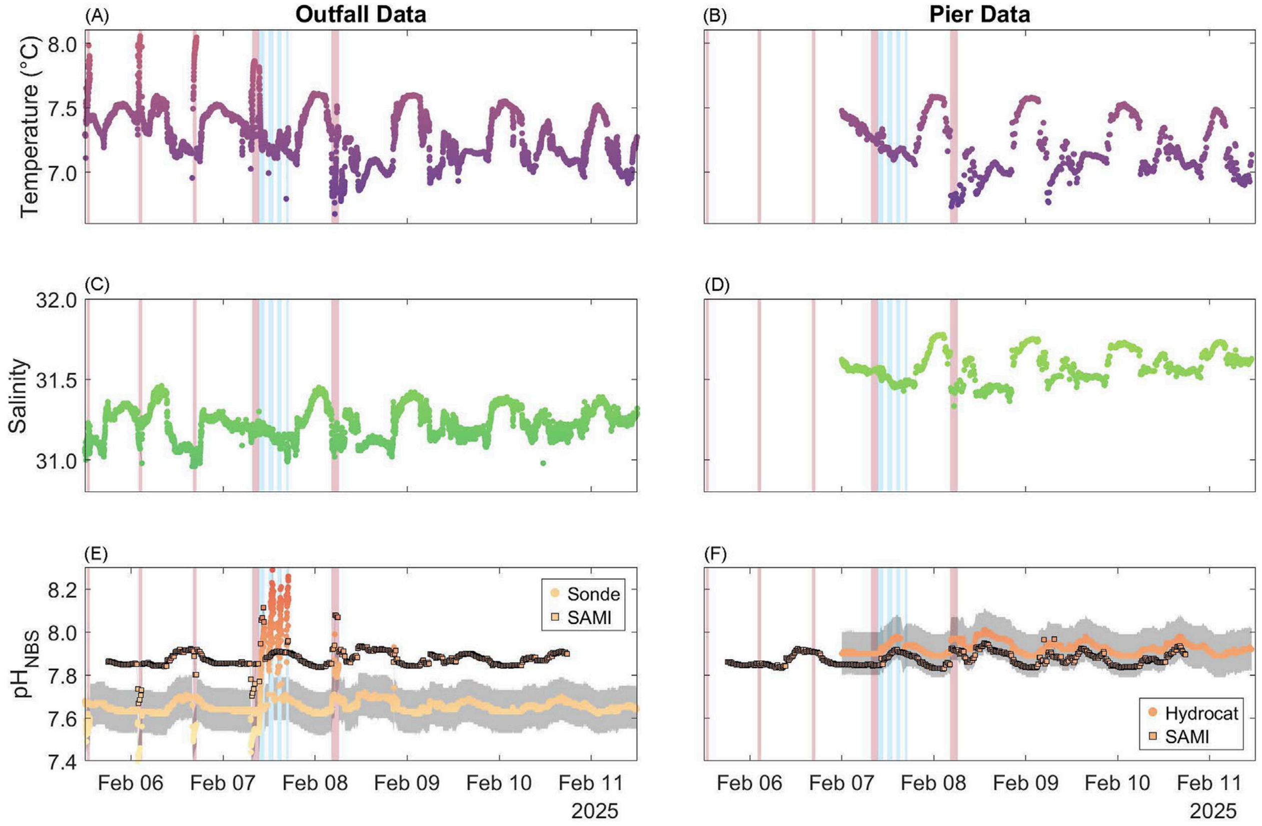

FIGURE 7
Data collected before, during, and after the February alkalinity release at the Outfall (left) and Pier (right) for Temperature **(A,B)**, salinity **(C,D)**, and pH_{NBS} **(E,F)**. Blue boxes indicate periods where alkalinity was discharged into Sequim Bay. Red boxes indicate the release of wastewater from the PNNL WWTP under normal operation (i.e., not related to these alkalinity release experiments).

alkalinity-enhanced seawater release and continuing for 4 days afterwards (Figure 7). The sensors at the outfall were positioned closer to the center line of flow from the outfall during the February release, which improved monitoring capabilities and allowed for the detection of the four pulses of increased pH (reaching a peak pH_{NBS} 8.3) (Figure 4). Ambient seawater pH_{NBS} ranged from 7.6–7.7. The YSI Exo 2 sonde recorded a higher peak pH_{NBS} (8.3) than that of the SAMI-pH (8.1), which only captured an increase in pH during the first and fourth pulsed releases from the WWTP due to the reduced measurement frequency (15 min) and perhaps slightly different positioning relative to the outfall (Figures 6, 7). The YSI Exo2 sonde was in the direct line of the outfall plume compared to the SAMI, which is slightly higher in the water column (Figure 4). In addition, current speeds were faster during the second release than the first, which may have diluted the pH signal more quickly and made it more difficult to capture (Supplementary Figure S12). The pH rapidly returned to ambient values between pulses, ranging from 7.4–7.7 via YSI sonde or 7.7–7.9 via SAMI-pH (Figures 6, 7). No shift in pH was measured by either the SAMI-pH or Seabird Hydrocat EP-V2 at the nearby pier during or after the alkaline releases (Supplementary Figures S7, S6, S11). SAMI-pH and Seabird Hydrocat data had strong agreement in pH_{NBS} measurements with one another as well as with the discrete samples collected off the pier (Table 2; Figures 6, 7). The higher accuracy of both the SAMI-pH and discrete sample data relative to the Seabird Hydrocat or YSI sonde, along with agreement between the pier sensor and sample data, indicate that the pH measurements made with the YSI sondes are biased low by 0.1–0.3 pH (Table 2). The high frequency variability in pH during the alkalinity-enhanced seawater discharges demonstrates the need for frequent sampling or continuous records, while the differing sensitivity of the SAMI-pH and YSI sonde pH records to the discharges likely reflects the strong heterogeneity of the impacts of any point source release into an energetic mixing environment. The differing accuracy and performance of these sensors versus sampling resolution demonstrates that the choice of sensor in a field experiment can matter greatly.

The treatment process of the seawater to enhance alkalinity did not appear to affect the temperature for the February release (Table 2). While higher temperatures were observed during the release period, they were not outside of those observed naturally in the system (Figure 7). There was also no measured increase in salinity associated with the alkalinity release compared to the natural variability of salinity in this system (Figure 7). The opposite trend was observed instead, where salinity decreased slightly throughout the day on February 7 at both the outfall and pier (Figure 7). The salinity at the pier does appear to be slightly higher than the outfall, which could be due to multiple factors. The first is that the use of different sensors led to an offset, however, it is unlikely that this would lead to an offset of 0.5. The second is that the pier is slightly closer to the inlet for the Bay from the Salish Sea, resulting in higher

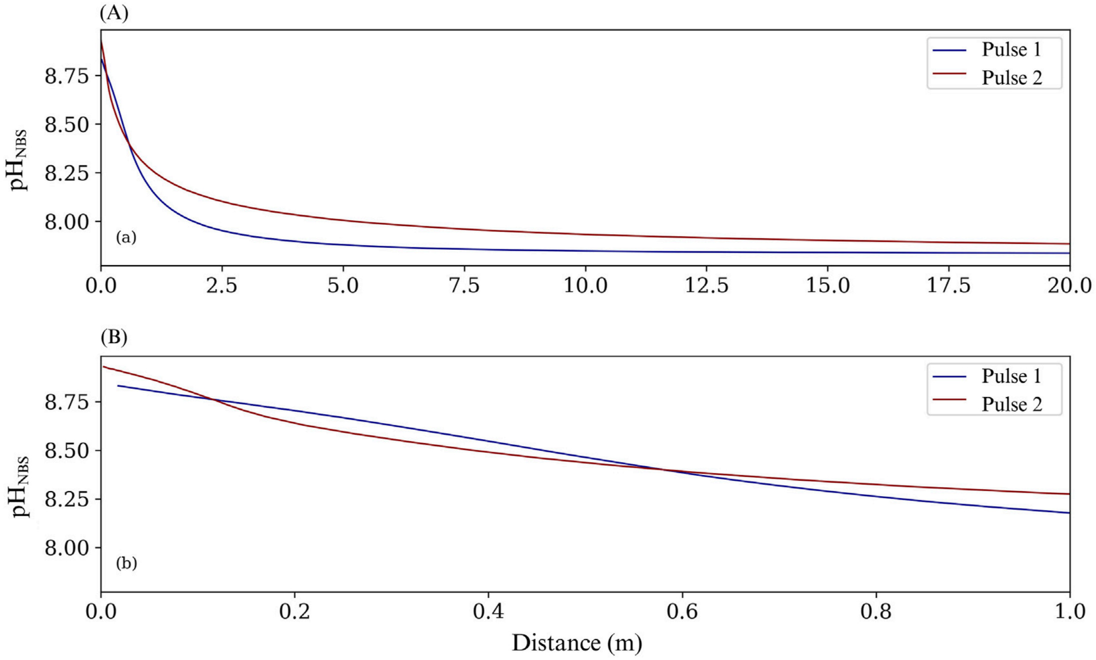

FIGURE 8
Variation of pH_{NBS} along the plume trajectory over a **(A)** 20 m distance from the outfall and **(B)** within 1 m distance from the outfall as indicated via PLUMES2.0.

salinities. The third is that under normal WWTP operation, the salinity of the released water is slightly fresher than the surrounding water, considering it receives both fresh and saline water from PNNL facilities (Figures 4, 7). When analyzing the pH_{NBS} at the pier station over the week, there is a small increase during the discharge event, however, it is not significantly different from the average pH_{NBS} conditions occurring naturally within the system over this period (Figures 6, 7). Therefore, the alkalinity-enhanced seawater released at the outfall was likely diluted quickly near the outfall and did not affect the nearby pier station (Figure 7). This is further supported by the PLUMES2.0 model, which demonstrated that the pH signal dissipates within approximately 2.5 m from the outfall (Figure 8). In addition, strong currents near the outfall in Sequim Bay would promote mixing and dilution of the pH signal (Supplementary Figure S12). Before the alkalinity release, there were four regular wastewater releases from the WWTP that released warmer, less salty, and lower pH water to the Bay (Figure 7). Following the alkalinity release, there was a release from the WWTP on February 8 that released both wastewater from the labs as well as residual alkalinity treated water that was still in the GW Cells, which explains the peak in pH during this period (Figure 7). There were not any other releases recorded in this time series following the release on February 8 due to unrelated facility mechanical problems.

4 Discussion

These field trials demonstrated the ability to release electrochemically generated alkalinity through an existing, pre-permitted coastal outfall with minimal to barely detectable influence on local water conditions. pH_{NBS} was successfully measured and controlled throughout the wastewater treatment system to ensure that pH of the effluent was limited to <9.0. There was minimal impact on water temperature and salinity while elevating the pH within the permitted thresholds (Figure 7). During normal WWTP operations, water has a longer residence time within the laboratory facilities, providing opportunities for water in the system to heat or cool relative to ambient seawater. During the February field trial, however, our continuous pumping of water substantially decreased this residence time, minimizing thermal differences between the discharge and receiving waters of Sequim Bay. It is important to note that the brine product stream was not added to the final released product in this study due to logistical reasons. Therefore, we did not expect to see shifts in salinity relative to natural seawater conditions during these releases. However, even if the brine product was reintroduced with the base product, it is unlikely that we could detect a signal due to its relatively small volume compared to the large volume of seawater it is diluted in (approximately only 0.2% of total volume).

The improved detection of alkalinity-enhanced seawater in February at the outfall was primarily due to a more optimal positioning of the sensors relative to the direct flow of the outfall (Figure 4) but may also be partly due to the larger volume of the alkalinity release in February compared to November (Figure 3). The difference between the two field trials in November and February demonstrates that even when the discharge volume increased by over 6-fold, there was still only limited detectability of increased pH to just outside the outfall pipe (Figures 5–7). In either case, the difference between ambient and OAE pH conditions is relatively small and may be difficult to capture beyond the outfall for MRV purposes (Figures 6, 7). Positioning sensors precisely within the direct flow of an outfall is logistically challenging, requiring divers to deploy a cage attached to the outfall, and optimal placement of sensors may vary with tidal conditions. Capturing the signal of a plume further from the outfall in a dynamic tidal system like Sequim Bay is even more challenging without a substantially larger treatment (i.e., higher pH and volume). These logistical and observational challenges highlight the need for modeling to support MRV, particularly for smaller-scale experiments and deployments.

During both field trials, there was no measured increase in pH_{NBS} by either the SAMI-pH or Hydrocat sensors at the nearby pier (Figures 5, 6). One possible reason for this is that the sensors installed at the pier station may not have been optimally positioned to capture the plume despite the fact that outgoing tides during the February experiment should have directed the plume towards the pier. However, based on data from the PLUMES2.0 model, the pH signal from the plume dissipates quickly within 2.5 m from the outfall due to fast dilution of the alkalinity-enhanced seawater by currents in this area (Figure 8; Supplementary Figure S12). These data, along with PLUMES2.0 simulations, indicate that the problem for detection was not necessarily sensor placements but the scale of the alkalinity release. Releasing seawater with higher alkalinity concentrations may increase the distance of detectability further from the outfall to allow for measurements further away (Figure 8). However, there is a potential tradeoff between the increased measurability of the plume and the increased localized impact of the alkalinity addition.

Evaluation of the above tradeoffs should include clear definition of research questions in the context of an OAE deployment, the range of natural variability in pH and carbonate chemistry inherent to a field site, and consideration of both potential positive and negative impacts of shifts in pH and carbonate chemistry on the marine communities that may be present within the perturbed volume of seawater around the outfall. We note that increasing the pH and alkalinity of the effluent also requires consideration of the potential for secondary precipitation of carbonate minerals, which is dependent on factors including temperature, salinity, carbonate chemistry, and suspended solids in the water column (Mucci, 1983; Zhong and Mucci, 1989; Pan et al., 2021; Wurgaft et al., 2021; Fuhr et al., 2022; Hartmann et al., 2023; Paul et al., 2024; Ringham et al., 2024; Suitner et al., 2024; Varliero et al., 2024). While many laboratory studies have investigated this precipitation, which is linked to both inefficiencies in alkalinity delivery and potential impacts on marine biology associated with increasing turbidity, there are few examples of methods for quantifying precipitation in OAE field studies (Moras et al., 2022). Therefore, where alkalinity is released under conditions approaching potential secondary precipitation thresholds, and until precipitation thresholds are better defined, we recommend collecting continuous measurements near the outfall for both carbonate chemistry and turbidity. It is important to note that most marketed turbidity sensors currently have an accuracy between 1% (Seabird) to 2% (YSI), which can still translate to relatively large error given the range in detectability (0–4000 NTU). Therefore, special care should be taken during calibration and data quality control checks. Still, these data will be useful for demonstrating compliance with water quality regulations, validating dilution models, and evaluating the impact of the alkalinity-enhanced seawater discharge on the local marine environment. Based on current literature, OAE has mixed impacts on marine species, even within individual groups of calcifiers (Ferderer et al., 2022; Gately et al., 2023; Jones et al., 2024; Bednaršek et al., 2025; Britton et al., 2025). For these field trials, we were unable to collect data to assess the impacts of the alkalinity-enhanced seawater delivered to the local marine species. However, we hypothesize that only organisms within direct proximity to the outfall would be impacted based on the limited extent and duration of the plume, along with the lack of evidence of secondary precipitation *in situ*.

The data from the PLUMES2.0 model exemplifies the value of leveraging near-field modeling capabilities to help inform field deployment strategies alongside regional ocean models used to quantify carbon removal resulting from OAE. Models can be used to build a better observation network by simulating a large number of model scenarios to explore when and where the best detectability occurs. As a result, we can develop a better MRV system for mCDR which is essential for the advancement of the technology. For example, the impact of tidal currents on the alkaline plume may limit detection by the deployed sensors. High-resolution forecasts of local current conditions could help inform stationary sensor placement for field trials. Likewise, model simulations could be used to program spatially-resolved monitoring routes by automated vehicles to track plumes in greater detail in more offshore waters. While PLUMES2.0 was used post-experiment to understand plume dynamics based on field data, it could very well be used in the future to determine the range of detectability from the outfall for future trials. In addition, broader regional models can help with tracking alkalinity plumes. The elevated pH and alkalinity and decreased pCO_2 resulting from alkalinity-enhanced seawater addition in these plumes may be measurable at the outfall, however CO_2 removal and storage occur over the timescales of air-sea equilibration in the broader oceanographic region (Jones et al., 2014; Bach et al., 2023; Ho et al., 2023; Wang et al., 2023). Measurement, reporting, and verification (MRV) for OAE must then rely on the combination of direct measurement of the rate and concentration of the alkalinity-enhanced seawater returned to the surface ocean, direct measurement of water quality parameters in the immediate vicinity of the outfall for permit compliance and impact monitoring, and ocean modeling to quantify carbon removal and storage (Fennel et al., 2023; Ho et al., 2023). Both near-field and regional model outputs can help inform field sensor deployment, which in turn would allow for better measurement of the alkalinity release for MRV and regulatory purposes. These models could also be used to help determine if a site is a viable option for OAE deployment based on local currents and tides. Laboratory experiments can supplement this work and provide insights into OAE by building a body of knowledge to assess the safety and viability of OAE in advance of field trials. Lab experiments can better capture processes that are not currently measurable due to signal-to-noise issues at the current scale of small field trials and help develop operational guidelines for MRV to improve our ability to evaluate the safety and efficacy of OAE, especially those focused around secondary precipitation kinetics and biological responses to OAE (Bach et al., 2023; Ho et al., 2023; Iglesias-Rodríguez et al., 2023; Riebesell et al., 2023; Bednaršek et al., 2025).

In summary, we leveraged existing outfall permits for the WWTP at PNNL-Sequim to release alkalinity-enhanced seawater within cautious pH thresholds, which is likely how operators with existing outfall permits (e.g., WWTPs, desalination plants, etc.) would approach early adoption of OAE deployments. However, other mCDR studies have shown that under similar seawater temperature and salinity conditions, we could release seawater at increased alkalinity and pH conditions (+1,400 µmol/kg and ~9.5, respectively) with limited risk of secondary precipitation of carbonate minerals, particularly in regions where alkalinity-enhanced seawater discharges would be rapidly diluted into the surrounding environment (Suitner et al., 2024; Suitner et al., 2025). It is important to note that this is true for the alkaline feedstock used in this study and may not be applicable to other forms of alkaline feedstock. For example, lower precipitation thresholds have been observed when using solid mineral dispersal versus aqueous solutions, likely due to the increased number of precipitation nuclei (Moras et al., 2022; Hartmann et al., 2023; Moras et al., 2024; Suitner et al., 2024). The facilities at PNNL-Sequim could be leveraged for further field testing and significant advancements in mCDR research with appropriate discharge permits that allow for the release of increased alkalinity-enhanced seawater. The WWTP at PNNL-Sequim is relatively small compared to typical municipal water treatment facilities in Washington state that may operate at >1,000x the capacity of this facility. A quick calculation based on the volume of alkalinity output by the PNNL facility during the February field trial release indicated that the amount of alkalinity released (~251 mol NaOH) could account for about 8.9 kg of equivalent CO_2 for this one experiment, based on the conversion of ~0.8 mol CO_2 captured per mol alkalinity released in the form of NaOH (Wang et al., 2023; Khangaonkar et al., 2024; Ringham et al., 2024). Daily repetition of this experiment over the course of a year could result in sequestration of ~3.2 metric tons of CO_2 per year, which is about 70% of the yearly emissions from one typical US car (US EPA, 2025). The Ebb Carbon BPMED system at PNNL-Sequim could produce enough NaOH to sequester ~100 tons of CO2 per year, enough to offset around ~22 cars per year (US EPA, 2025). However, discharge of this volume of alkalized seawater is constrained by our capacity for onsite dilution to allow for release of an effluent $pH_{NBS} < 9.0$. While PNNL-Sequim's WWTP would need permits that allow for release at higher pH to have a broader impact in carbon removal, it has high value as a research and development test bed in OAE.

Paired with larger WWTP or industrial facilities that discharge large volumes of seawater, electrochemically derived aqueous alkalinity provides a valid approach among many in the CDR toolbox. Even if constrained to release seawater of $pH_{NBS} < 9.0$, the release of alkalinity-enhanced seawater from larger facilities would begin to increase ocean carbon uptake and regionally offset ocean acidification (Khangaonkar et al., 2024). However, we note that there is a disconnect between the intention of NPDES permits, namely, to regulate, control, and minimize the impact of pollutants on the natural environment, and the intention of OAE, which is to perturb the natural environment through the addition of alkalinity (Steenkamp and Webb, 2023). While some NPDES permits may technically allow for OAE, we cannot extrapolate this work to imply that all NPDES-permitted outfalls will be allowed to intentionally discharge alkalinity (Murthy et al., 2025). It is also important to note the disconnect between pH reporting between these two communities. From a regulatory standpoint, the NBS scale for pH is commonly output by the lower cost sensors and reported for compliance and monitoring purposes. However, the researchers studying mCDR OAE or ocean acidification typically report on total scale, as it is commonly measured by oceanographic instruments. This is necessary to keep in mind for future research experiments in OAE so that results are communicated accurately to the regulatory community.

We recommend that future research should continue to refine constraints, monitoring, and modeling approaches for ocean alkalinity enhancement that enhance the growing body of research. Field demonstrations of alkaline releases can be leveraged to more easily acquire appropriate NPDES permits for OAE deployment at coastal facilities in the future, such as that of Ebb Carbon's upcoming research pilot with an increased effluent pH limit in Port Angeles, WA. This work will allow for greater scaling in OAE field trials, which could be useful for integrating these systems with coastal facilities going forward. When possible, high-accuracy continuous measurements should be utilized near the outfall for field trials, however, we recognize that this may not be sustainable for regular compliance at many facilities. Therefore, calibration and comparison with discrete samples should be done at regular intervals when using less accurate but more cost-efficient sensors to account for any offset between the two. In addition, we think this study would have benefitted from additional post-deployment calibration checks and recommend them for future field work campaigns. Finally, we emphasize that the limits of detection of alkaline signals in dynamic coastal environments require improvement in both dilution modeling, to assess the movement and potential near-field impacts of alkaline plumes, and regional modeling, to quantify resulting carbon dioxide removal. These tools are already valuable for OAE MRV, however, improving parameterizations of variables like secondary precipitation and gas transfer velocity for air-sea gas exchange would improve their accuracy. The field of mCDR and OAE is quickly expanding, and we hope that the rapid reporting of this work can help inform the community as new research evolves.

Data availability statement

A project page has been created on NOAA's NCEI database under the title "Data for Novel field trial for ocean alkalinity enhancement using electrochemically derived aqueous alkalinity from 2024-11-07 to 2025-02-08 (NCEI Accession 0307424)" and is accessible at https://www.ncei.noaa.gov/archive/accession/0307424.

Author contributions

AS: Validation, Visualization, Formal Analysis, Data curation, Writing – review and editing, Writing – original draft. MR: Validation, Methodology, Writing – review and editing, Visualization, Investigation, Supervision, Formal Analysis, Resources, Writing – original draft. CT: Formal Analysis, Writing – review and editing, Investigation, Validation. BC: Writing – review and editing, Investigation, Supervision, Funding acquisition, Resources, Project administration, Conceptualization, Methodology. SD: Writing – review and editing, Data curation. RF: Funding acquisition, Conceptualization, Writing – review and editing, Supervision. DH: Writing – review and editing. JH: Writing – review and editing. TK: Software, Writing – review and editing, Methodology. JL: Writing – original draft, Visualization, Methodology, Writing – review and editing. TM:

Writing – review and editing, Supervision, Methodology. TP: Writing – review and editing. LP: Validation, Writing – original draft, Writing – review and editing, Formal Analysis, Visualization. CS: Funding acquisition, Project administration, Writing – review and editing. JV: Writing – review and editing. NW: Funding acquisition, Project administration, Conceptualization, Supervision, Writing – review and editing, Investigation, Methodology.

Funding

The author(s) declare that financial support was received for the research and/or publication of this article. This study was led by Pacific Northwest National Laboratory, which is operated for the US Department of Energy by Battelle Memorial Institute under contract DE-AC05-76RL01830. Financial support for this research was provided by the US Department of Energy's Water Power Technologies Office Laboratory Research Program, the Climateworks Foundation Grant Number 22–2361, and the National Oceanographic Partnership Program (NOPP) under the National Oceanic and Atmospheric Administration's Ocean Acidification Program (Crossref Funder ID: 100018228; ROR ID: https://ror.org/02bfn4816) award to University of Washington CICOES. The CICOES and PMEL contributions are numbers 2025–1456 and 5778, respectively. Production of the alkaline feedstock was carried out by Ebb Carbon, which also financially supported MR, DH, JL, TM, TP, and JV

Acknowledgments

We acknowledge Matthew Eisaman's substantial and invaluable contributions to this project, and regret that he passed before seeing the final dataset. We greatly appreciated the efforts by the PNNL facilities personnel and divers who deployed the sensors at the outfall.

Conflict of interest

Authors MR, DH, JL, TM, TP, and JV were employed by Ebb Carbon, Inc.

The remaining authors declare that the research was conducted in the absence of any commercial or financial relationships that could be construed as a potential conflict of interest.

Generative AI statement

The author(s) declare that no Generative AI was used in the creation of this manuscript.

Publisher's note

Supplementary material

The Supplementary Material for this article can be found online at: https://www.frontiersin.org/articles/10.3389/fenve.2025.1641277/full#supplementary-material

References

Albright, R., Caldeira, L., Hosfelt, J., Kwiatkowski, L., Maclaren, J. K., Mason, B. M., et al. (2016). Reversal of ocean acidification enhances net coral reef calcification. *Nature* 531, 362–365. doi:10.1038/nature17155

Anderson, H. J., Mongin, M., and Matear, R. J. (2025). Ocean alkalinity enhancement in a coastal channel: simulating localised dispersion, carbon sequestration and ecosystem impact. *Environ. Res. Commun.* 7, 041012. doi:10.1088/2515-7620/adce5a

Bach, L. T., Ho, D. T., Boyd, P. W., and Tyka, M. D. (2023). Toward a consensus framework to evaluate air–sea $_{\mathrm{CO2}}$ equilibration for marine $_{\mathrm{CO2}}$ removal. *Limnol. Oceanogr. Lett.* 8, 685–691. doi:10.1002/lol2.10330

Bach, L. T., Ferderer, A. J., Laroche, J., and Schulz, K. G. (2024). Technical note: Ocean alkalinity enhancement pelagic impact intercomparison project (OAEPIIP). *Biogeosciences* 21, 3665–3676. doi:10.5194/bg-21-3665-2024

Baumgartner, D. J., Frick, W. E., and Roberts, P. J. W. (1994). *Dilution models for effluent discharges*. Washington, D.C.: Office of Research and Development, US Environmental Protection Agency.

Bednaršek, N., Van De Mortel, H., Pelletier, G., García-Reyes, M., Feely, R. A., and Dickson, A. G. (2025). Assessment framework to predict sensitivity of marine calcifiers to ocean alkalinity enhancement – identification of biological thresholds and importance of precautionary principle. *Biogeosciences* 22, 473–498. doi:10.5194/bg-22-473-2025

Britton, D., Visch, W., and Bach, L. T. (2025). Moderate ocean alkalinity enhancement likely to have minimal effects on a habitat-forming kelp across multiple life stages. *Limnol. Oceanogr.* 70, 1283–1295. doi:10.1002/lno.70029

Cai, W.-J., and Jiao, N. (2022). Wastewater alkalinity addition as a novel approach for ocean negative carbon emissions. *Innovation* 3, 100272. doi:10.1016/j.xinn.2022.100272

Cai, W.-J., Wang, Y., and Hodson, R. E. (1998). Acid-base properties of dissolved organic matter in the estuarine waters of Georgia, USA. *Geochimica Cosmochimica Acta* 62, 473–483. doi:10.1016/s0016-7037(97)00363-3

Campbell, K., Weekes, C., Evans, W., Gimenez, I., and Hales, B. (2023). *Hakai institute's Burke-o-Lator TCO2/pCO2 analyzer discrete sample analysis protocols (V2.0)*. Hakai Institute. doi:10.21966/1.521066

Carbon to sea intiative (2024). Community-driven workshop advances OAE data management guidelines. Available online at: https://carbontosea.org/2024/12/18/agu-oae-workshop/(Accessed March 06, 2025).

Carbon to sea intiative (2025). Carbon to sea Co-Sponsors workshop to lay the groundwork for African oCDR road map. Available online at: https://carbontosea.org/2025/04/29/african-ocdr-road-map-workshop/(Accessed March 06, 2025).

Cong, H.-T., Yan, X.-Q., Yang, L.-K., Jiang, Y., Wang, C., Zhan, D., et al. (2024). Coupling electrochemical alkalinization and mineral dissolution for ambient removal of both influent CO2 and dissolved nitrite in seawater. *Environ. Sci. and Technol. Lett.* 11, 546–552. doi:10.1021/acs.estlett.4c00313

Cross, J. N., Sweeney, C., Jewett, E. B., Feely, R. A., Mcelhany, P., Carter, B., et al. (2023). *Strategy for NOAA carbon dioxide removal (CDR) research: a white paper documenting a potential NOAA CDR science strategy as an element of NOAA's climate interventions portfolio*.

Cross, J. N., Geerlofs, S. H., Subban, C. V., Ward, N. D., Meinig, C., Pinza, M. R., et al. (2024). *Towards marine carbon dioxide removal (mCDR) centers of excellence*. Richland, WA, United States: Pacific Northwest National Laboratory.

Degrandpre, M. D., Hammar, T. R., Smith, S. P., and Sayles, F. L. (1995). *In situ* measurements of seawater pCO2. *Limnol. Oceanogr.* 40, 969–975. doi:10.4319/lo.1995.40.5.0969

Dickson, A. G. (1990). Standard potential of the reaction:, and and the standard acidity constant of the ion HSO4− in synthetic sea water from 273.15 to 318.15 K. *J. Chem. Thermodyn.* 22, 113–127. doi:10.1016/0021-9614(90)90074-z

Dickson, A. G., Sabine, C. L., and Christian, J. R. (2007). *Guide to best practices for ocean CO2 measurements*, 3. PICES Special Publication, 191. doi:10.25607/OBP-1342

Eisaman, M. D. (2024). Pathways for marine carbon dioxide removal using electrochemical acid-base generation. *Front. Clim.* 6, 1349604. doi:10.3389/fclim.2024.1349604

Eisaman, M. D., Parajuly, K., Tuganov, A., Eldershaw, C., Chang, N., and Littau, K. A. (2012). CO2 extraction from seawater using bipolar membrane electrodialysis. *Energy and Environ. Sci.* 5, 7346–7352. doi:10.1039/c2ee03393c

Eisaman, M. D., Geilert, S., Renforth, P., Bastianini, L., Campbell, J., Dale, A. W., et al. (2023). Assessing the technical aspects of ocean-alkalinity-enhancement approaches. *State Planet* 2-oae2023, 1–29. doi:10.5194/sp-2-oae2023-3-2023

Evans, W., Pocock, K., Hare, A., Weekes, C., Hales, B., Jackson, J., et al. (2019). Marine CO2 patterns in the northern Salish Sea. *Front. Mar. Sci.* 5, 536. doi:10.3389/fmars.2018.00536

Fassbender, A. J., Alin, S. R., Feely, R. A., Sutton, A. J., Newton, J. A., and Byrne, R. H. (2017). Estimating total alkalinity in the Washington state coastal zone: complexities and surprising utility for ocean acidification research. *Estuaries Coasts* 40, 404–418. doi:10.1007/s12237-016-0168-z

Fennel, K., Long, M. C., Algar, C., Carter, B., Keller, D., Laurent, A., et al. (2023). Modelling considerations for research on ocean alkalinity enhancement (OAE). *State Planet* 2-oae2023, 1–29. doi:10.5194/sp-2-oae2023-9-2023

Ferderer, A., Chase, Z., Kennedy, F., Schulz, K. G., and Bach, L. T. (2022). Assessing the influence of ocean alkalinity enhancement on a coastal phytoplankton community. *Biogeosciences* 19, 5375–5399. doi:10.5194/bg-19-5375-2022

Ferderer, A., Schulz, K. G., Riebesell, U., Baker, K. G., Chase, Z., and Bach, L. T. (2024). Investigating the effect of silicate- and calcium-based ocean alkalinity enhancement on diatom silicification. *Biogeosciences* 21, 2777–2794. doi:10.5194/bg-21-2777-2024

Fuhr, M., Geilert, S., Schmidt, M., Liebetrau, V., Vogt, C., Ledwig, B., et al. (2022). Kinetics of olivine weathering in seawater: an experimental study. *Front. Clim.* 4, 831587. doi:10.3389/fclim.2022.831587

Gately, J. A., Kim, S. M., Jin, B., Brzezinski, M. A., and Iglesias-Rodriguez, M. D. (2023). Coccolithophores and diatoms resilient to ocean alkalinity enhancement: a glimpse of hope? *Sci. Adv.* 9, eadg6066. doi:10.1126/sciadv.adg6066

Harding, S. F., and Harker-Klimes, G. E. (2017). *Field measurement of velocity time series in the center of sequim Bay*. Richland, WA, United States: Pacific Northwest National Lab.

Hartmann, J., Suitner, N., Lim, C., Schneider, J., Marín-Samper, L., Arístegui, J., et al. (2023). Stability of alkalinity in ocean alkalinity enhancement (OAE) approaches – consequences for durability of CO2 storage. *Biogeosciences* 20, 781–802. doi:10.5194/bg-20-781-2023

Hashim, M., Marx, L., Klein, F., Dean, C., Burdige, E., Hayden, M., et al. (2025). Mineral formation during shipboard ocean alkalinity enhancement experiments in the north Atlantic. *EGUsphere* 2025, 1–31. doi:10.5194/egusphere-2025-988

He, J., and Tyka, M. D. (2023). Limits and CO2equilibration of near-coast alkalinity enhancement. *Biogeosciences* 20, 27–43. doi:10.5194/bg-20-27-2023

Hibbeln, C. F., Marsh, P., Myers, C. R., Valdez, P. J., Edmundson, S. J., and Subban, C. V. (2024). Maximizing marine carbon removal by coupling electrochemical and biological methods. *Environ. Sci. and Technol. Lett.* 11, 438–444. doi:10.1021/acs.estlett.4c00107

Ho, D. T., Bopp, L., Palter, J. B., Long, M. C., Boyd, P. W., Neukermans, G., et al. (2023). Monitoring, reporting, and verification for ocean alkalinity enhancement. *State Planet* 2-oae2023, 1–12. doi:10.5194/sp-2-oae2023-12-2023

ICES (2025). Workshop on marine carbon dioxide removal (WKmCDR; outputs from 2024 meeting). *ICES Sci. Rep*. doi:10.17895/ices.pub.28246358.v3

Iglesias-Rodríguez, M. D., Rickaby, R. E. M., Singh, A., and Gately, J. A. (2023). Laboratory experiments in ocean alkalinity enhancement research. *Guide Best Pract. Ocean Alkalinity Enhanc. Res.* 2-oae2023, 5. doi:10.5194/sp-2-oae2023-5-2023

IPCC (2018). "IPCC, 2018: summary for policymakers," in *Global warming of 1.5°C. An IPCC special report on the impacts of global warming of 1.5°C above pre-industrial levels and related global greenhouse gas emission pathways, in the context of strengthening the global response to the threat of climate change, sustainable development, and efforts to eradicate poverty*. Editors Masson-Delmotte, V., Zhai, P., Pörtner, H.-O., Roberts, D., Skea, J., and Shukla, P. R. (Cambridge, UK: Cambridge University Press).

IPCC (2023). "IPCC, 2023: climate change 2023: synthesis report," in *Contribution of working groups I, II and III to the sixth assessment report of the intergovernmental panel on climate change*. Editors Team, C. W., Lee, H., and Romero, J. (Generva, Switzerland: IPCC).

Jones, D. C., Ito, T., Takano, Y., and Hsu, W. C. (2014). Spatial and seasonal variability of the air-sea equilibration timescale of carbon dioxide. *Glob. Biogeochem. Cycles* 28, 1163–1178. doi:10.1002/2014gb004813

Jones, M. E., Pinza, M. R., and Southard, S. S. (2019). *Operational planning strategy for a sequim Bay underwater UXO test site (SBU2)*. Richland, WA, United States: Pacific Northwest National Lab. doi:10.5194/bg-22-1615-2025

Jones, K., Hemery, L., Ward, N., Regier, P., Ringham, M., and Eisaman, M. (2024). Biological response of eelgrass epifauna, Taylor's sea hare (Phyllaplysia taylori) and eelgrass isopod (idotea resecata), to elevated ocean alkalinity. *EGUsphere* 2024, 1–25.

Khangaonkar, T., Carter, B. R., Premathilake, L., Yun, S. K., Ni, W., Stoll, M. M., et al. (2024). Mixing and dilution controls on marine CO2 removal using alkalinity enhancement. *Environ. Res. Lett.* 19, 104039. doi:10.1088/1748-9326/ad7521

Kulkarni, T., Yang, B., Zhang, X., Kumar, R., and Arges, C. G. (2024). ACS spotlight: bipolar membranes for electrochemical energy conversion, chemical manufacturing, and separations. *ACS Appl. Energy Mater.* 7, 11361–11389. doi:10.1021/acsaem.3c03260

Lai, C.-Z., Degrandpre, M. D., and Darlington, R. C. (2018). Autonomous optofluidic chemical analyzers for marine applications: insights from the submersible autonomous moored instruments (SAMI) for pH and pCO2. *Front. Mar. Sci.* 4, 438. doi:10.3389/fmars.2017.00438

Lee, K., Kim, T.-W., Byrne, R. H., Millero, F. J., Feely, R. A., and Liu, Y.-M. (2010). The universal ratio of boron to chlorinity for the north Pacific and north Atlantic oceans. *Geochimica Cosmochimica Acta* 74, 1801–1811. doi:10.1016/j.gca.2009.12.027

Lueker, T. J., Dickson, A. G., and Keeling, C. D. (2000). Ocean pCO2 calculated from dissolved inorganic carbon, alkalinity, and equations for K1 and K2: validation based on laboratory measurements of CO2 in gas and seawater at equilibrium. *Mar. Chem.* 70, 105–119. doi:10.1016/s0304-4203(00)00022-0

Montserrat, F., Renforth, P., Hartmann, J., Leermakers, M., Knops, P., and Meysman, F. J. (2017). Olivine dissolution in seawater: implications for CO(2) sequestration through enhanced weathering in coastal environments. *Environ. Sci. Technol.* 51, 3960–3972. doi:10.1021/acs.est.6b05942

Moras, C. A., Bach, L. T., Cyronak, T., Joannes-Boyau, R., and Schulz, K. G. (2022). Ocean alkalinity enhancement – avoiding runaway CaCO3 precipitation during quick and hydrated lime dissolution. *Biogeosciences* 19, 3537–3557. doi:10.5194/bg-19-3537-2022

Moras, C. A., Cyronak, T., Bach, L. T., Joannes-Boyau, R., and Schulz, K. G. (2024). Effects of grain size and seawater salinity on magnesium hydroxide dissolution and secondary calcium carbonate precipitation kinetics: implications for ocean alkalinity enhancement. *Biogeosciences* 21, 3463–3475. doi:10.5194/bg-21-3463-2024

Mucci, A. (1983). The solubility of calcite and aragonite in seawater at various salinities, temperatures, and one atmosphere total pressure. *Am. J. Sci.* 283, 780–799. doi:10.2475/ajs.283.7.780

Murthy, A., Silverman-Roati, K., and Webb, R. M. (2025). Regulation of ocean alkalinity enhancement in Washington state. *SABIN Cent. Clim. CHANGE LAW*. Available online at: https://scholarship.law.columbia.edu/sabin_climate_change/242.

National Academies of Sciences and Medicine (2022). *A research strategy for ocean-based carbon dioxide removal and sequestration*. Washington, DC: The National Academies Press.

Oschlies, A., Bach, L. T., Rickaby, R. E. M., Satterfield, T., Webb, R., and Gattuso, J.-P. (2023). Climate targets, carbon dioxide removal, and the potential role of ocean alkalinity enhancement. *State Planet* 2-oae2023, 1–9. doi:10.5194/sp-2-oae2023-1-2023

Palter, J. B., Cross, J. N., Long, M. C., Rafter, P. A., and Reimers, C. E. (2023). The science we need to assess marine carbon dioxide removal. *Eos* 104. doi:10.1029/2023eo230214

Pan, Y., Li, Y., Ma, Q., He, H., Wang, S., Sun, Z., et al. (2021). The role of Mg2+ in inhibiting CaCO3 precipitation from seawater. *Mar. Chem.* 237, 104036. doi:10.1016/j.marchem.2021.104036

Paul, A. J., Haunost, M., Goldenberg, S. U., Hartmann, J., Sánchez, N., Schneider, J., et al. (2024). Ocean alkalinity enhancement in an open ocean ecosystem: biogeochemical responses and carbon storage durability. *EGUsphere* 2024, 1–31. doi:10.5194/bg-22-2749-2025

Pawlowicz, R. (2020). *M_Map: a mapping package for MATLAB*. 1.4m ed.

Perez, F. F., and Fraga, F. (1987). The pH measurements in seawater on the NBS scale. *Mar. Chem.* 21, 315–327. doi:10.1016/0304-4203(87)90054-5

Rau, G. H. (2011). CO2 mitigation *via* capture and chemical conversion in seawater. *Environ. Sci. and Technol.* 45, 1088–1092. doi:10.1021/es102671x

Renforth, P., and Henderson, G. (2017). Assessing ocean alkalinity for carbon sequestration. *Rev. Geophys.* 55, 636–674. doi:10.1002/2016rg000533

Riebesell, U., Basso, D., Geilert, S., Dale, A. W., and Kreuzburg, M. (2023). Mesocosm experiments in ocean alkalinity enhancement research. *State Planet* 2-oae2023, 1–14. doi:10.5194/sp-2-oae2023-6-2023

Ringham, M. C., Hirtle, N., Shaw, C., Lu, X., Herndon, J., Carter, B. R., et al. (2024). An assessment of ocean alkalinity enhancement using aqueous hydroxides: kinetics, efficiency, and precipitation thresholds. *Biogeosciences* 21, 3551–3570. doi:10.5194/bg-21-3551-2024

Roberts, P. J. W. (1990). *Outfall design considerations*. New York, USA: John Wiley and Sons, Ltd.

Rogelj, J., Popp, A., Calvin, K. V., Luderer, G., Emmerling, J., Gernaat, D., et al. (2018). Scenarios towards limiting global mean temperature increase below 1.5 °C. *Nat. Clim. Change* 8, 325–332. doi:10.1038/s41558-018-0091-3

Schulz, K. G., Bach, L. T., and Dickson, A. G. (2023). Seawater carbonate chemistry considerations for ocean alkalinity enhancement research: theory, measurements, and calculations. *State Planet* 2-oae2023, 1–14. doi:10.5194/sp-2-oae2023-2-2023

Seidel, M. P., Degrandpre, M. D., and Dickson, A. G. (2008). A sensor for *in situ* indicator-based measurements of seawater pH. *Mar. Chem.* 109, 18–28. doi:10.1016/j.marchem.2007.11.013

Sharp, J. D., and Byrne, R. H. (2021). Technical note: excess alkalinity in carbonate system reference materials. *Mar. Chem.* 233, 103965. doi:10.1016/j.marchem.2021.103965

Sharp, J. D., Pierrot, D., Humphreys, M. P., Epitalon, J.-M., Orr, J. C., Lewis, E. R., et al. (2020). *CO2SYSv3 for MATLAB*. Zenodo. doi:10.5281/ZENODO.3950563

Steenkamp, R. C., and Webb, R. (2023). Legal considerations relevant to research on ocean alkalinity enhancement. *State Planet* 2-oae2023, 1–19. doi:10.5194/sp-2-oae2023-10-2023

Subhas, A., Michel, A., Wang, A. Z., Rheuban, J. E., Kim, H. H., Chen, K., et al. (2024). "Introducing the LOC-NESS project and results from LOC-01, our first tracer release experiment," in Ocean Sciences Meeting, New Orleans, LA, 18-23 February 2024.

Suitner, N., Faucher, G., Lim, C., Schneider, J., Moras, C. A., Riebesell, U., et al. (2024). Ocean alkalinity enhancement approaches and the predictability of runaway precipitation processes: results of an experimental study to determine critical alkalinity ranges for safe and sustainable application scenarios. *Biogeosciences* 21, 4587–4604. doi:10.5194/bg-21-4587-2024

Suitner, N., Hartmann, J., Varliero, S., Faucher, G., Suessle, P., and Moras, C. A. (2025). Surface area and Ω-aragonite oversaturation as controls of the runaway precipitation process in ocean alkalinity enhancement. *EGUsphere* 2025, 1–26. doi:10.5194/egusphere-2025-381

Sutton, A. J., Sabine, C. L., Maenner-Jones, S., Lawrence-Slavas, N., Meinig, C., Feely, R. A., et al. (2014). A high-frequency atmospheric and seawater $p\mathrm{CO}_2$ data set from 14 open-ocean sites using a moored autonomous system. *Earth Syst. Sci. Data* 6, 353–366. doi:10.5194/essd-6-353-2014

Thyng, K. M., Greene, C. A., Hetland, R. D., Zimmerle, H. M., and Dimarco, S. F. (2016). True colors of oceanography: guidelines for effective and accurate colormap selection. *Oceanography* 29, 9–13. doi:10.5670/oceanog.2016.66

Travis, K. (2025). Cross-sector recommendations to advance mCDR science in California. Available online at: https://www.oceansciencetrust.org/stories/mcdrworkshop2024/(Accessed May 16, 2025).

UN (2015). *Paris agreement*.

US EPA (2021). Chinook salmon. Available online at: https://www.epa.gov/salish-sea/chinook-salmon#:~:text=The%20Salish%20Sea%20is%20home,dog%20salmon%3B%20Oncorhynchus%20keta.

US EPA (2025). Greenhouse gas emissions from a typical passenger vehicle. Available online at: https://www.epa.gov/greenvehicles/greenhouse-gas-emissions-typical-passenger-vehicle.

Varliero, S., Buono, A., Caserini, S., Raos, G., and Macchi, P. (2024). Chemical aspect of ocean liming for CO2 removal: dissolution kinetics of calcium hydroxide in seawater. *ACS Eng. Au* 4, 422–431. doi:10.1021/acsengineeringau.4c00008

Wang, H., Pilcher, D. J., Kearney, K. A., Cross, J. N., Shugart, O. M., Eisaman, M. D., et al. (2023). Simulated impact of ocean alkalinity enhancement on atmospheric CO2 removal in the Bering Sea. *Earth's Future* 11, e2022EF002816. doi:10.1029/2022ef002816

Wurgaft, E., Wang, Z. A., Churchill, J. H., Dellapenna, T., Song, S., Du, J., et al. (2021). Particle triggered reactions as an important mechanism of alkalinity and inorganic carbon removal in river plumes. *Geophys. Res. Lett.* 48, e2021GL093178. doi:10.1029/2021gl093178

Yankovsky, E., Zhou, M., Tyka, M., Bachman, S., Ho, D., Karspeck, A., et al. (2024). Impulse response functions as a framework for quantifying ocean-based carbon dioxide removal. *EGUsphere* 2024, 1–26. doi:10.5194/egusphere-2024-2697

Yao, W., Morganti, T. M., Wu, J., Borchers, M., Anschütz, A., Bednarz, L., et al. (2025). Exploring site-specific carbon dioxide removal options with storage or sequestration in the marine environment – the 10 Mt CO2 yr−1 removal challenge for Germany. *Earth's Future* 13, e2024EF004902. doi:10.1029/2024ef004902

Zhong, S., and Mucci, A. (1989). Calcite and aragonite precipitation from seawater solutions of various salinities: precipitation rates and overgrowth compositions. *Chem. Geol.* 78, 283–299. doi:10.1016/0009-2541(89)90064-8

Zhou, M., Tyka, M. D., Bachman, S., Yankovsky, E., Karspeck, A. R., Ho, D. T., et al. (2024). "A global efficiency map of ocean alkalinity enhancement (OAE) for CO2 removal," in EGU General Assembly 2024, Vienna, Austria, 14–19 Apr 2024.